Available online at www.sciencedirect.com
ScienceDirect
Coordination Chemistry Reviews 252 (2008) 1287–1314
COORDINATION CHEMISTRY REVIEWS
www.elsevier.com/locate/ccr

Review

Silenes: Connectors between classical alkenes and nonclassical heavy alkenes

Henrik Ottosson *, Anders M. Eklöf

Department of Biochemistry and Organic Chemistry, Box 576, Uppsala University, 751 23 Uppsala, Sweden

Received 2 January 2007; accepted 19 July 2007
Available online 25 July 2007

Contents

Abstract

Forty years have passed since the first publication of the experimental evidence for formation of a Si=C double bonded compound, a silene. Since then, a large number of transient as well as isolable silenes have been studied, both experimentally and theoretically. Herein, we focus on the impact of the substituents on the electronic and geometric structure, reactivity, and other properties of (formally) Si=C double bonded compounds. Qualitative quantum chemical models for the bonding are reviewed, and applied to rationalize experimental observations. Silenes can have planar (classical) structures similar to alkenes, or nonplanar (nonclassical) structures similar to the heavier alkene congeners, and their

* Corresponding author.
E-mail address: henrik.ottosson@biorg.uu.se (H. Ottosson).

doi:10.1016/j.ccr.2007.07.005

substituents are pivotal in determining which of these structures is adopted. Silene properties, ranging from charge distribution and NMR chemical shifts to reactivities, are strongly connected to the electronic structure of the silene, and thus to its substitution pattern.

Keywords: Silenes; Heavy alkenes; Substituent effects; MO theory; Silicon; Structure and reactivity

1. Introduction

With double bonds between one carbon atom and one silicon atom, silenes are compounds that link the properties of alkenes with those of their heavier congeners. Naively viewed, silenes are half organic and half inorganic, and thus represent good connectors between classical organic chemistry and classical main group inorganic chemistry. It is often the substituents of a silene that determine its properties, for instance whether its structure is similar to that of planar alkenes or to those of the nonplanar heavier congeners, and this will be the focus of the present review. Several comprehensive reviews have previously been written on the topic of silenes [1]. The present review contains an update of the field, and is predominantly focused on the impact of the substituents on the properties of silenes.

The chemistry of silenes has been an active research area ever since Gusel'nikov and Flowers in 1967 reported the first evidence for the existence of a silene (1,1-dimethylsilene **2**, Scheme 1) as a transient intermediate in the pyrolysis of silacyclobutane **1** [2]. In 1981, Brook and co-workers reported the formation of the first isolable silene (**5a**, Scheme 2) that was persistent at room temperature [3], and this triggered further research in the area of main group multiply bonded compounds. Since then, a variety of different investigations have been performed, predominantly on the fundamental properties of silenes, and the field has now gradually become more mature for applications. The work of Steel and co-workers on the use of silenes as novel reagents in stereoselective organic synthesis provide good examples of such applications [4], and the very early study by Bertrand et al. on asymmetric induction at Si from prochiral silenes is potentially interesting in similar regards [5]. It has also been pointed out that the incorporation of Si into bioactive molecules can provide distinct advantages in terms of higher activity and better pharmacokinetic profiles [6], and facile and selective cycloaddition reactions involving silenes could offer efficient routes to such cyclic Si-containing bioactive molecules. Detailed studies of the various substituent effects in silenes are important to the search for silenes that can be widely applied in synthesis [7]. Silenes that react selectively, that are less air and moisture sensitive than most silenes, that do not dimerize, and that are easily accessible, are desirable for organic synthesis [8].

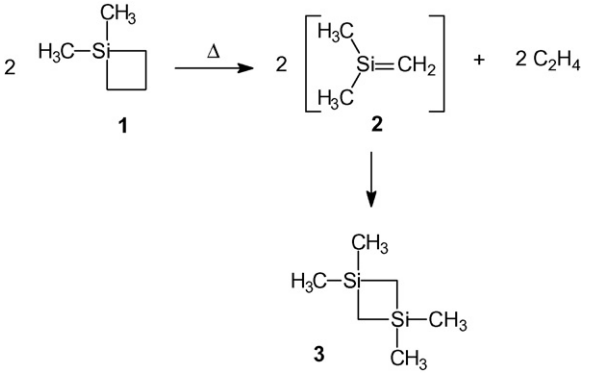

Scheme 1.

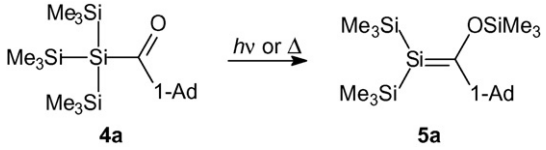

Scheme 2.

This review focuses on the effect of substituents on the geometry, reactivity, and other properties that are related to the electronic structure of silenes. The cumulative experience on how to tune the properties of silenes through their substituents provides a very valuable tool for developing their applications. We have selected Si=C bonded compounds that exemplify the effects of the substituents, and therefore, not all investigated Si=C bonded compounds are covered in this review.

2. Properties of the parent silene $H_2Si{=}CH_2$

To assess the effect of the substituents it is necessary to first discuss the properties of the parent silene, $H_2Si{=}CH_2$ (**6**). This species is planar with C_{2v} symmetry. Complete sets of bond lengths and angles for seven different isotopomers of this compound were determined by Bailleux et al. through millimeter and submillimeter wave spectroscopy [9]. The Si=C bond length was determined as 1.7039(18) Å, and a distance of 1.7045 Å was found at CCSD(T)/cc-pV(Q,T)Z level. The C–H and Si–H bond lengths are 1.0819(12) and 1.4671(9) Å, respectively, and the HCSi and HSiC bond angles are 122.00(4)° and 122.39(3)°, revealing sp^2 hybridized C and Si atoms. The strength of the π-bond of **6** is calculated to be in the range 37–54 kcal/mol, depending on computational method used [10–12]. This is approximately 57–83% of the π-bond strength of a regular C=C double bond (65 kcal/mol in ethylene [13]).

The calculated dipole moment of **6** is 0.693 D at CCSD(T)/cc-pV(Q,T)Z level [14]. This $Si^{\delta+}{=}C^{\delta-}$ polarity, referred to as the natural silene polarity, is in line with what can be expected based on the electronegativities of Si and C. The charge distribution correlates with the NMR chemical shifts because the ^{13}C and ^{29}Si NMR chemical shifts calculated at the GIAO-MP2/tz2p(Si,C)dzp(H)//B3LYP/6-311+G(2df,p) level of theory are 105.3 and 53.8 ppm, respectively [15]. The C atom is thus more shielded than the one in ethylene, where a ^{13}C NMR chemical shift of 123.5 ppm is reported [16].

The parent silene was isolated at 10 K in an Ar matrix and studied by IR and UV spectroscopy [17]. An IR band at 985 cm^{-1} was assigned to the Si=C bond stretch vibration, indicating that the Si=C bond is weaker than a regular C=C bond. Moreover, the UV spectrum of $H_2Si{=}CH_2$ has an absorption maximum that corresponds to the $\pi\pi^*$ transition at 258 nm [17], and which is redshifted by approximately 100 nm when compared to ethylene [18]. Its first ionization potential is 8.9 eV [19], which is 1.6 eV less than that of ethylene [20].

3. Theory and computations of the Si=C bond

Qualitative models are often useful when describing the effect of substituents, and especially when describing the geometric structure of substituted silenes. Several different models can be applied to understand this bonding, including Lappert's original donor–acceptor model, the Carter–Goddard–Malrieu–Trinquier model, and models based on second-order Jahn–Teller distortions. After an outline of the major qualitative models, we rationalize substituent effects using them. The models are often general for alkenes and heavy alkenes; therefore in this section we do not focus solely on silene studies. More quantitative quantum chemical calculations of the Si=C bond, and in particular the effect of substituents on the bonding, will also be discussed.

3.1. Qualitative models for the E=E′ bond (E = E′ = Group 14 element)

Lappert and co-workers isolated and structurally characterized the first heavy alkene, distannene **7** (Scheme 3) [21]. The X-ray structure determination of **7** revealed that the Sn atoms are markedly pyramidal ($\sum\alpha(Sn) = 342^\circ$) so that the distannene adopts a *trans*-bent structure. The original interpretation of the bonding in the nonplanar structure was in terms of a double donor–acceptor bond (A, Scheme 4), or alternatively, a valence bond description (B) [21,22]. The latter explanation was furthered by Pauling who concluded that the SnSn bond in **7** is best described as a single covalent bond involving two sp^3 hybrid orbitals and an unshared electron pair resonating between the fourth sp^3 hybrid orbital of each of the two tin atoms [23].

In the late 1970s, Volland, Davidson, and Borden analyzed the extent to which second-order Jahn–Teller (SOJT) effects influence the shape of the potential energy surface that describes the simultaneous pyramidalization of the two C atoms in ethylene [24,25]. This process leads to either *cis*- or *trans*-bent structures, and provides for orbital stabilization as the symmetry reduction allows mixing of the empty σ^* and filled π MOs (Scheme 5). It was noted that such mixings, and consequently the SOJT distortions, become more important as Group 14 is descended because of smaller energy differences between the occupied and unoccupied orbitals, and this was proposed to explain the *trans*-bent structure of Lappert's distannene [24].

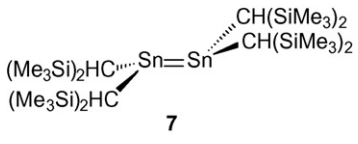

7

Scheme 3.

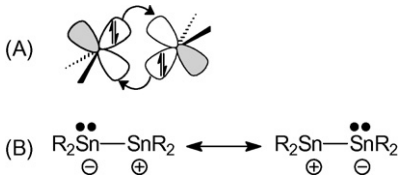

Scheme 4.

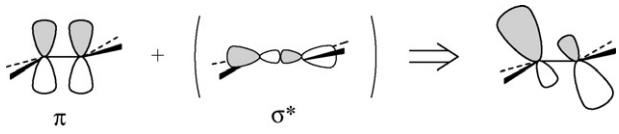

Scheme 5.

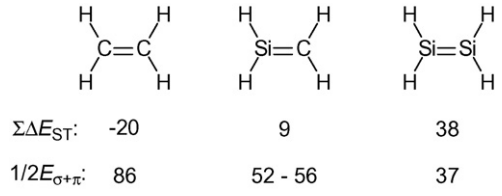

Fig. 1. Calculated sums of the singlet–triplet energy gaps ($\sum\Delta E_{ST}$) of the two interacting H_2E and H_2E' species and the total bond strength ($E_{\sigma+\pi}$) of an $H_2E{=}E'H_2$ molecule. Energies in kcal/mol from Ref. [29].

A different line of analysis of the Group 14 E=E′ double bond was started when Carter and Goddard rationalized the variation in C=C bond strengths in substituted alkenes in terms of the singlet–triplet energy splittings (ΔE_{ST}) of two interacting carbene fragments [26]. It was shown that the C=C bond strength of a substituted alkene $D(XYC{=}CX'Y')$ is simply the intrinsic C=C bond energy $D_{int}(C{=}C)$ taken as the dissociation energy of ethylene (172 ± 2 kcal/mol) [27], minus the sum of ΔE_{ST} of the two carbene fragments (Eq. (3.1)). For the tetrafluoroethylene the value predicted using this formula is in excellent agreement with the measured value ($D^{pred} = 79 \pm 2$ kcal/mol [26] and $D^{exp} = 76.3 \pm 3$ kcal/mol [28]).

$$D(XYC{=}CX'Y') = D_{int}(C{=}C) - [\Delta E_{ST}(CXY) + \Delta E_{ST}(CX'Y')] \quad (3.1)$$

Trinquier and Malrieu developed this theory to cover also the structural variations that exist among heavy alkenes, and focused on explaining when a heavy alkene adopts a planar structure and when it adopts a *trans*-bent nonplanar structure [29]. Today, this theory is known as Carter–Goddard–Malrieu–Trinquier (CGMT) theory. An energetic boundary for the onset of *trans*-bending in a homonuclear $H_2E{=}EH_2$ alkene is provided by the inequality $\sum\Delta E_{ST} \geq 1/2E_{\sigma+\pi}$ which is derived from VB theory. In this equation $E_{\sigma+\pi}$ is the total bond strength of the E=E double bond, and *trans*-bending sets in when the inequality holds. The validity can be exemplified by $H_2C{=}CH_2$, $H_2Si{=}CH_2$, and $H_2Si{=}SiH_2$ (Fig. 1). For ethylene, which is a truly planar molecule, the sign of $\sum\Delta E_{ST}$ is even opposite to that of the half of the total double bond strength. For the parent

silene, $\sum\Delta E_{ST}$ and $1/2E_{\sigma+\pi}$ have the same sign but $\sum\Delta E_{ST}$ is much smaller than half the Si=C bond strength. However, for the parent disilene the two energetic entities are very similar, and disilenes are species that can adopt classical planar as well as nonclassical bent structures [30]. As we will see shortly, this also applies to substituted silenes as they can adopt both types of structures; one planar structure and one structure with the Si atom pyramidalized. Because the ΔE_{ST} of carbenes as well as of silylenes vary extensively with substitution, it is apparent from CGMT theory that the structures of substituted silenes as a result will vary widely ranging from classical to nonclassical structures [31]. Indeed, the *trans*-bending angle θ for a homonuclear H_2EEH_2 species can be predicted from the $\Delta E_{ST}/E_{\sigma+\pi}$ ratio using Eq. (3.2) [32].

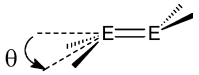

$$\theta = \arccos(2 - 4\Delta E_{ST}/E_{\sigma+\pi}) \quad (3.2)$$

Therefore, closely linked with the nonplanar structures of heavy alkenes, including silenes, is thus the fact that all heavy carbenes R_2E: (E=Si–Pb), with one exception [33], have singlet–multiplicity ground states [34]. The reason for this was recently analyzed by Apeloig, Chapman, and co-workers through decomposition of the CASSCF energies of the singlet and triplet states of CH_2 and SiH_2 [35]. Whereas the ΔE_{ST} of CH_2 is −9 kcal/mol favoring the triplet state, it is 20 kcal/mol in SiH_2 with the singlet state being lowest. The difference (∼60%) in ΔE_{ST} stems predominantly from differences in electron–electron repulsion between the frontier electrons, which is larger in the singlet state of CH_2 than SiH_2 because of the smaller size of the sp^2(C) as compared to the sp^2(Si) hybrid orbital. The reduction in this repulsion when going from the singlet to the triplet state is therefore largest for CH_2:

$$\Delta E_{TBE} = \Delta E_{snap} - \Delta E_{prep} = \Delta E_{snap} - \Delta E^{e}_{prep} - \Delta E^{g}_{prep} \quad (3.3)$$

TBE is the total bond energy.

$$\Delta E_{snap} = \Delta E_{elstat} + \Delta E_{Pauli} + \sum_{\Gamma}\Delta E^{\Gamma}_{int} \quad (3.4)$$

Using density functional theory (DFT) Jacobsen and Ziegler (JZ) decomposed the bonding energy of the E=E double bond into various contributions (Eqs. (3.3) and (3.4), and Fig. 2) [36]. The total bond strength of an $H_2EE'H_2$ molecule composed of two (heavy) carbene fragments H_2E and H_2E' can be described as the energy gained by snapping together the triplet state H_2E and H_2E' heavy carbenes with the geometries that are optimal for $H_2EE'H_2$ (ΔE_{snap}), minus the energy required to prepare the H_2E and H_2E' species (ΔE_{prep}). The ΔE_{prep} has both an electronic part (excitation from the singlet ground state to the triplet state) as well as a geometric part (distortion from the optimal (singlet) ground state geometry to the geometry that the fragment adopts in $H_2EE'H_2$). With regard to ΔE_{snap}, it is composed of electrostatic attraction/repulsion (ΔE_{elstat}), Pauli (antisymmetry) repulsion (ΔE_{Pauli}), and attractive orbital interactions

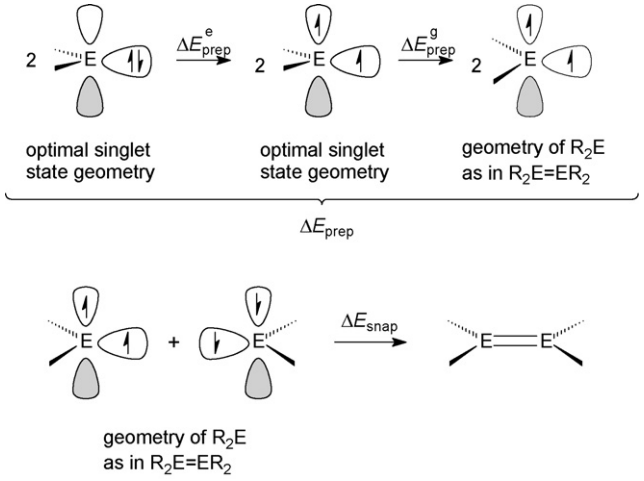

Fig. 2. Schematic drawing of the geometric and electronic changes that occur during formation of an $R_2E{=}ER_2$ molecule from two singlet ground state R_2E fragments.

($\sum\Delta E^{\Gamma}_{int}$). As ΔE_{snap} is higher than the ΔE_{prep}, a $H_2EE'H_2$ system is expected to be stable with an EE′ bond.

Himmel and Schnöckel continued along the lines of JZ, however, using a different terminology [37]. They divided the dissociation energy (ΔE_{diss}) of homonuclear H_2EEH_2 species into (i) a fragmentation part (ΔE_{frag}) which corresponds to the negative ΔE_{snap} of JZ, and (ii) a relaxation part (ΔE_{relax}) similar to $-\Delta E_{prep}$ by JZ. They find that classical bonds, where each H_2E fragment contributes one electron to the σ-bond and one electron to the π-bond, have smaller ΔE_{relax} for a triplet-state H_2E fragment than for the corresponding singlet-state fragment. The opposite applies for bonds that result from donor–acceptor interactions. Their calculations reveal that disilenes are *trans*-bent donor–acceptor species while alkenes are classically bonded. Silenes are thus at the borderline as they are composed of one carbene and one silylene fragment.

3.2. Bond strengths and bond orders

Early on Schmidt, Gordon, and Dupuis used MCSCF calculations to estimate the π-bond strengths of $H_2Si{=}CH_2$ [11]. Through twisting from the planar closed-shell equilibrium geometry to the perpendicularly twisted singlet biradical form, they found the π-bond strength to be 37 kcal/mol, i.e. 57% that of ethylene (65 kcal/mol [13]). Jacobsen and Ziegler used DFT to calculate an intrinsic π-bond energy of 54.5 kcal/mol based on the b_2 symmetric orbital interaction [36]. More recently, Shaik, Hiberty and co-workers investigated $H_mA = BH_n$ molecules with A and B = C, N, O, Si, P, and S, and applied a VB technique which leads to *in situ* π-bond energies with intact σ frameworks [12]. For $H_2Si{=}CH_2$ they find a π-bond energy of 47.1 kcal/mol, which is 65% that of ethylene (72.0 kcal/mol) at the same level of theory.

With regard to the total (σ + π) bond strength of the Si=C double bond it has been estimated computationally as 105–113 kcal/mol [38], and with the values above for the π-bond strength this leaves 56–76 kcal/mol for the σ-bond. However,

Si–C single bond strengths are normally ∼90 kcal/mol [39]. The nonadditivity can be rationalized by the divalent state stabilization energy (DSSE), a concept introduced by Walsh and co-workers [39,40]. In short, the DSSE measures the difference in first and second dissociation energy of an X_4E species, successively leading to X_3E and X_2E:. The second dissociation energy becomes progressively lower as the element E becomes heavier, reflecting an increased intramolecular stabilization of divalent species as Group 14 is descended. The DSSE also varies with substituent X (*vide infra*).

As noted above, Jacobsen and Ziegler derived the intrinsic σ- and π-bond strengths of unsubstituted heavy alkenes [36]. They concluded that the relative influence of the $b_u(\pi)$-bond in the total E=E bonding increases as the heavy alkene is distorted to a *trans*-bent structure. However, bond strengths can also be correlated with force constants. Grunenberg analyzed the compliance force constants of multiply bonded Si compounds, which in contrast to the real force constants, provide unique and complete descriptions of the bond strengths [41]. He found that pyramidalization at Si and *trans*-bending of SiC multiple bonds, such as in the parent silaacetylene HSi≡CH [42], markedly reduce the SiC bond strength, and lower the bond order from the maximal. When regarding the linear structures of H_3SiCH_3, H_2SiCH_2, and HSiCH, a clear linear increase in the compliance force constants was seen. This suggests that at the planar equilibrium structure of the parent silene, a true Si=C double bond is formed. However, the SiC bond in the C_{2h} symmetric bent equilibrium structure of HSiCH is not a true triple bond when judged from the compliance force constants. Distortions to nonclassical structures also occur in substituted silenes, and Grunenberg's findings suggest that such compounds do not have full Si=C double bonds.

Properties of the electron density can also be used to clarify the bonding in heavy alkenes. The electron localization function (ELF) represents the excess in kinetic energy caused by Pauli repulsion and gives a measure of the probability of finding two electrons with the same spin in a given space [43]. The ELF is defined to attain values between 0 and 1, where a high value (→1) shows on localization of an electron pair. The value of ELF of the uniform electron gas is everywhere 1/2. Using the ELF, Grützmacher and Fässler clarified the topographical similarities of the electron density of classical and nonclassical multiple bonds because ELF gradually transforms from classical bonds, categorized by them as unslipped bonds, to nonclassical bonds, categorized as slipped bonds [44]. In an unslipped double bond, the two local ELF maxima are placed symmetrically above and below the plane of the $H_2E{=}EH_2$ molecule, whereas for slipped (nonclassical) double bonds each maximum is shifted towards either of the two Group 14 atoms. Heavy alkenes were found to have slipped double bonds.

However, the analysis of Grützmacher and Fässler was criticized by Malcolm, Gillespie and Popelier, who besides ELF analysis also performed an AIM study (atoms-in-molecules [45]) of the heavy-alkene bond orders [46]. Their analysis was based on B3LYP/cc-pVDZ densities and revealed that caution must be exercised to the concept of slipped double bonds. The ELF analysis does not give quantitative values of bond orders; rather it indicates that for $H_2E{=}EH_2$ (E = Si, Ge or Sn) they are less than two and larger than one. The topological bond orders derived by AIM are more quantitative. A bond order of 1.2 is calculated for the parent disilene and similar values are found for the parent digermene and distannene. Malcolm, Gillispie, and Popelier attributed the decrease in bond order when compared to ethylene to a reduced ability of the less electronegative heavy Group 14 elements to attract electrons into the bonding region, whereby a part of the electron density remains nonbonding. Even though silenes were not analyzed, one can postulate that significant reductions in bond orders occur upon pyramidalizations of Si in these species.

3.3. Effects of substitution

It is known that π-donating and electronegative substituents stabilize the singlet state of carbenes and silylenes, whereas electropositive and bulky substituents stabilize the triplet state [47,48]. According to CGMT theory, the larger the ΔE_{ST} of the carbene and silylene fragments having singlet ground states, the more donor–acceptor character the silene will have. In CGMT theory, the formula $\sum \Delta E_{ST} \geq 1/2 E_{\sigma+\pi}$ for the onset of *trans*-bending in a substituted heavy alkene $X_2E{=}E'Y_2$ with π-donor substituents X and Y is expanded as in Eq. (3.5) [29]. In this equation, q_1 and q_2 are the net charges of the p_π AO's of the EX_2 and $E'Y_2$ fragments and α is a proportionality factor set to 212 kcal/mol. Using this formula Malrieu and Trinquier predict that $H_2Si{=}CF_2$ (**8**) will be slightly distorted from planarity, whereas $F_2Si{=}CF_2$ (**9**) will have a distinctly nonplanar structure:

$$\sum \Delta E_{ST} \geq \frac{1}{2} E_{\sigma+\pi} \left(1 + \frac{q_1 + q_2}{2}\right) + \alpha q_1 q_2 \tag{3.5}$$

Liang and Allen analyzed the significance of the SOJT effect in dependence of the substituent electronegativity [10]. They adopted a nuclear charge perturbation approach with which they simulated the effect of varying the electron-withdrawing ability of the substituents on the geometry of the E=E double bond (E = C, Si, Ge, or Sn). The nuclear charge of the hydrogen substituents (Z_H) was varied within $0.80 \leq Z_H \leq 1.05$ for E = Si, Ge and Sn, and within $0.80 \leq Z_H \leq 1.50$ for E = C. Thus, Z_H determines the electronegativity of the modified H atom. The C=C bonds stayed planar regardless of Z_H, whereas the disilene and the even heavier alkenes change geometry dramatically toward *trans*-bent as the nuclear charge Z_H increased. In conclusion, Liang and Allen showed that the geometries of the E=E bonds are determined both by their intrinsic π-σ* orbital energy separations, which enable SOJT effects of varying strengths, and the substituent electronegativity, which increases orbital mixing.

Rather recently, Gusel'nikov and co-workers investigated a series of $RR'Si{=}CH_2$ silenes (R and R′ = H, Me, SiH_3, CH_3O, NH_2, Cl, or F) with MP2 geometry optimizations and MP4 single-point energy calculations [49]. Their study connects to Liang and Allen's earlier conclusions because they find that $RR'Si{=}CH_2$ silenes with hydrogens at C are the heaviest alkenes in which electronegative substituents R and R′ do not distort the structure away from planarity. Indeed, $F_2Si{=}CH_2$ (**10**) is very near the breakpoint at which CGMT theory predicts that Si pyramidalization will set in [29].

Soon after the structural characterization of the first stable silene [3], Apeloig and Karni reported computational results of substituent effects in silenes [50]. Hartree–Fock (HF) calculations were performed on $RHSi{=}CH_2$ and $H_2Si{=}CHR$ silenes, where R = H, Me, SiH_3, F, OH, $OSiH_3$, CN or NO_2. They focused on the Si=C bond length, which for $H_2Si{=}CH_2$ (**6**) at HF/3-21G level was calculated as 1.717 Å, close to the more recent values of 1.7045 Å from CCSD(T)/cc-pV(Q,T)Z calculations and 1.7039 Å from millimeter wave spectroscopy [9]. For the substituted $RHSi{=}CH_2$ and $H_2Si{=}CHR$ silenes, the SiC bond length varied in the range 1.70–1.75 Å at HF/3-21G level. Substitution at Si shortened the Si=C bond relative to the parent silene, whereas substitution at C caused elongation, with the largest elongations found when R=OH and $OSiH_3$. Gusel'nikov and co-workers, as well as Cheng and Chu, recently observed the same trend for $RR'Si{=}CH_2$ silenes at the MP2 and B3LYP levels [49,51]. Indeed, Gusel'nikov and co-workers found a linear correlation between $r_{Si=C}$ and the Pauling electronegativity of the substituents R and R′ ($r = 0.968$).

The substituent effect on the Si=C bond length can be explained in terms of the Si=C bond polarity [50]. Electronegative substituents at Si will increase the natural inherent $Si^{\delta+}{=}C^{\delta-}$ polarity, increase the degree of bond ionicity, and as a result, shorten the bond [52]. In contrast, electronegative substituents at C decrease the negative charge at this atom, reduce the degree of bond ionicity, and consequently, give longer Si=C bonds. An MO theoretical description can also be given (Scheme 6). The valence AOs of Si are more diffuse than those of C, but an electron-withdrawing substituent at Si will contract its AOs, improve the bonding overlap with the AOs on C, and thereby shorten the bond. In contrast, an electron-withdrawing substituent at C will contract the already smaller AOs of C, reduce the orbital overlap with Si, and elongate the SiC bond. If the substituents at C are also π-donors, the resonance structures that place negative charge on Si (zwitterionic resonance structures

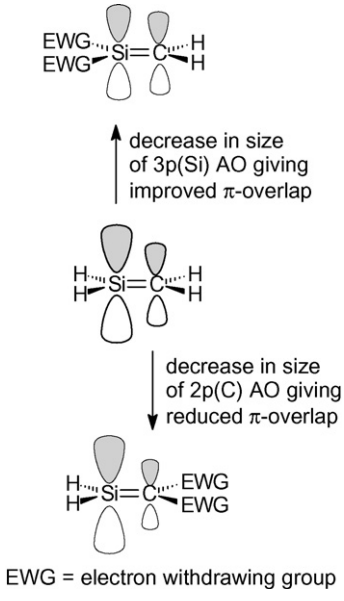

Scheme 6.

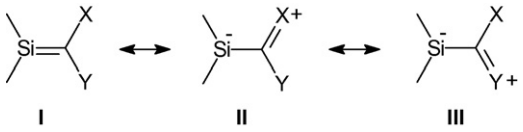

Scheme 7.

II and **III**, Scheme 7) will also play a role for the elongation of the Si=C bond. The more these resonance structures influence the electronic structure, the longer will the SiC bond become, and the more will the Si atom resemble that of a silyl anion. The pyramidalization of Si will thus increase with **II** and **III**. Consequently, the Si=C bond in Brook's silene **5a** was elongated relative to the parent silene by the electronic effects of the substituents, predominantly the $OSiMe_3$ group [3]. Notably, none of the monosubstituted silenes explored by Apeloig and Karni had a pyramidal structure around Si [50].

Fulvenes and fulvalenes are species that are influenced by aromaticity through dipolar resonance structures [53,54]. The triafulvene and its heterosubstituted analogues are particularly influenced by a resonance structure that places positive charge at the cyclopropenium ring and negative charge at the exocyclic position [55]. Lately, the Kira group experimentally and computationally investigated a series of 4-silatriafulvenes (Scheme 8) [56–58], and found the parent 4-silatriafulvene (**11**) on the borderline between a planar and a bent structure. The Si of **11** had an out-of-plane angle of 41.3°, even though the inversion barrier at Si (E_{inv}(Si)) was merely 1.4 kcal/mol at MP2/6-311++G(d,p)+ZPE level [57b]. The Kira group also computationally examined the structure and properties of a series of substituted 4-silatriafulvenes, and found that electronegative substituents at Si stabilized the bent structure whereas π-electron acceptors planarize the molecule, in line with Liang and Allen's earlier conclusions [10]. The E_{inv}(Si) was as high as 10.4 kcal/mol in 4,4-difluoro-4-silatriafulvene (**12**), whereas silyl substituents at Si lower E_{inv}(Si). An analogy can be drawn to silyl anions. Even though the trifluorosilyl anion has a $\sum\alpha$(Si) similar to that of the parent silyl anion (290.0° and 285.2°, respectively, at B3LYP/6-311+G(d,p) level), the E_{inv} of the former is much higher (54.6 and 25.3 kcal/mol at the same level of computation) [59–61], in line with the calculated E_{inv} values for **11** and **12**. Interestingly, the E_{inv} correlated with the charge distribution of the Si=C bond as measured by q(Si) and q(C) [57c]. Indeed, with regard to 4,4-disilyl-substituted 4-silatriafulvenes, a planar structure was observed by X-ray crystallography for an isolable 4-silatriafulvene [58]. In contrast, with fluoro substituents at Si the formal Si=C bond was nearly 0.2 Å longer than in the unsubstituted species (Fig. 3), and the Si became more pyramidal. The substituents at Si also impacted the aromaticity of 4-silatriafulvenes and significantly changed the Si=C π-bond strength [57b]. Interestingly, both

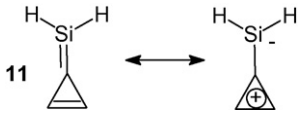

Scheme 8.

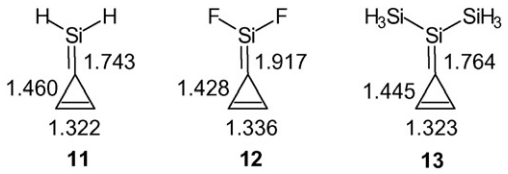

Fig. 3. Optimal bond lengths (Å) of the parent and substituted 4-silatriafulvenes calculated at the MP2/6-311++G(d,p) level. Values from Ref. [57b].

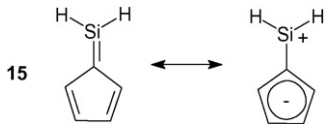

Scheme 9.

the λ_{max} in UV–vis spectra and the ^{29}Si NMR chemical shifts varied significantly when going from planar to pyramidal 4-silatriafulvenes according to GIAO ab initio NMR chemical shift calculations.

Saebø, Pittman and co-workers computationally explored the family of next-largest fulvene, pentafulvene (**14**), replacing the exocyclic C atom by Si, Ge or Sn (Scheme 9) [62]. In the silicon congener, the influence of the aromatic resonance structure causes a greater positive charge at Si, as compared to the parent silene. According to B3LYP calculations, the importance of this resonance structure was greater in 6-silapentafulvene (**15**) than in the all-C pentafulvene, and as a consequence, the CC bond length alternation in the ring was reduced slightly. With fluoro substituents attached to Si, nucleus independent chemical shifts indicated that the 6,6-difluoro-6-silapentafulvene (**16**) became somewhat more aromatic [62b,63].

Ottosson performed a computational study on the effects of increasingly reversed Si=C bond polarity, as measured by the charge at the Si atom (q(Si)), on the structural properties of silenes [64]. Silenes of the general type $Z_2Si{=}CXY$ (Z = H, Me or H_3Si; X = H, SH, Cl, F, OH or NH_2; Y = H, SH, Cl, F, OH, NH_2, O^-, S^- or NH^-) were investigated. This study built on Apeloig and Karni's concept of reversed Si=C bond polarization [50]. With the most strongly donating groups X and Y at C, the Si=C double bond was fully transformed into a long Si–C single bond and the Si atom became as pyramidal as it is in a silyl anion, even when Z=H (Fig. 4). Thus, in contrast to substitution at Si [49], substitution at C is able to rendered silenes very nonplanar and nonclassical structures. In all of these compounds, it is noteworthy that the C atom remained essentially planar. The geometric features of species such as $H_2Si{=}C(NH_2)_2$ (**19**)

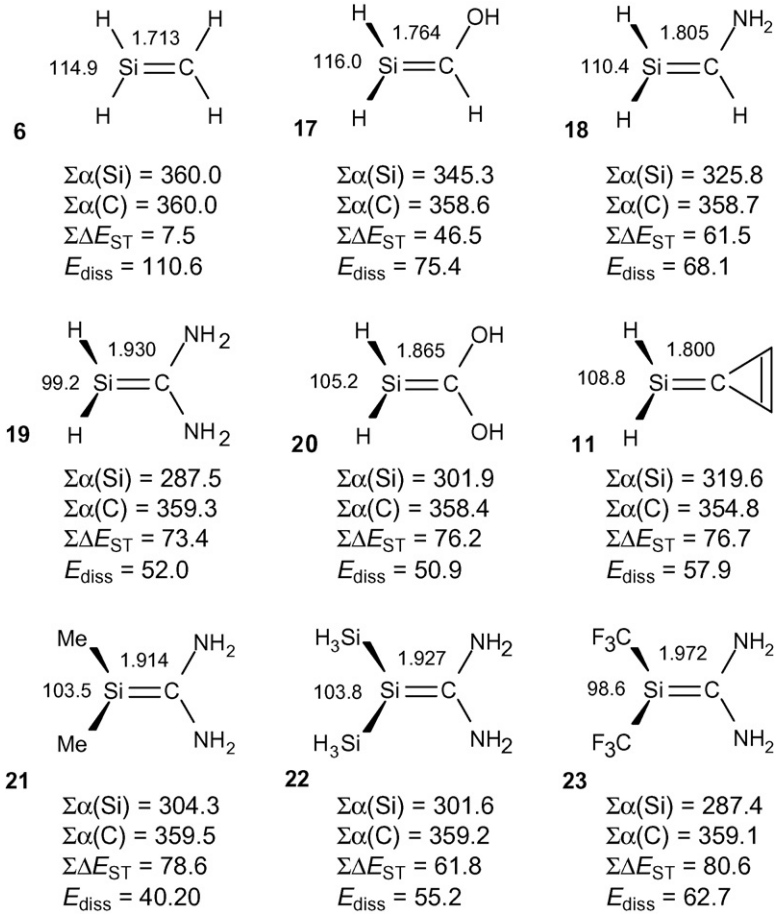

Fig. 4. Optimal bond distances and sum of valence angles at Si and C ($\sum\alpha$(Si) and $\sum\alpha$(C)) of selected silenes at B3LYP/6-31+G(d) level, together with calculated dissociation energies (E_{diss}), and sum of singlet–triplet energy gaps ($\sum E_{ST}$). Distances in Å, angles in °, and energies in kcal/mol. Values from Ref. [64].

suggested that zwitterionic resonance structures with negative charge at Si and positive at the C side were dominant.

A plot of the Si=C bond length versus q(Si) of the various Si=C bonded compounds revealed two linear parts separated by a breakpoint at which Si pyramidalization sets in [64]. The breakpoint corresponded approximately to the point where $\sum\Delta E_{ST} \approx f(E_{\sigma+\pi})$ according to Eq. (3.5) [64]. Moreover, for the Z_2Si=CXY silenes of Ottosson, the $\sum\Delta E_{ST}$ correlated with the bond dissociation energy E_{diss}, similar as Carter and Goddard found for substituted alkenes [26]. This also applied to the DSSE which correlated perfectly with the $\sum\Delta E_{ST}$. Indeed, the DSSE depends strongly on the electronegativity of the substituents at the divalent center [65]. Qualitatively, the dependence can be explained by the fact that more electronegative substituents will attract the bonding electrons further away from the Si nucleus and thus increase the attraction of the Si nucleus for its lone-pair electrons. This leads to an increased value of the DSSE [65a].

Very recently, Cheng and Chu published a quantum chemical B3LYP/cc-pVDZ study of disubstituted silenes similar to those investigated by Ottosson [64], but augmented to include silenes that contained $Si(NH)_2(CH)_2$ and/or $C(NH)_2(CH)_2$ cycles [51]. An interesting observation was that the geometries of the SiH_2 fragments of H_2Si=CXY silenes with planar equilibrium geometries was similar to the optimal geometry of triplet state SiH_2. On the other hand, in the silenes with pyramidal Si the SiH_2 fragment had a geometry that more resembled that of singlet state SiH_2. This relates to the finding of Himmel and Schnöckel that ΔE_{relax} (or similarly ΔE_{prep}) can be used to distinguish between (nonclassical) donor–acceptor bonded H_2EEH_2 species and (classical) $\sigma+\pi$ bonded species [37]. Cheng and Chu also found that π-donor substituents at C effectively raise the empty $2p_\pi$ MO of the carbene fragment, which leads to a raise in the energy of the π MO of the silene, thus reducing the energy gap between the π and σ* MO's (Fig. 5). A smaller πσ* gap lead to a more effective SOJT mixing and a stronger driving force for bending towards a nonclassical structure, in line with Vollard, Davidson and Borden's earlier conclusion [24].

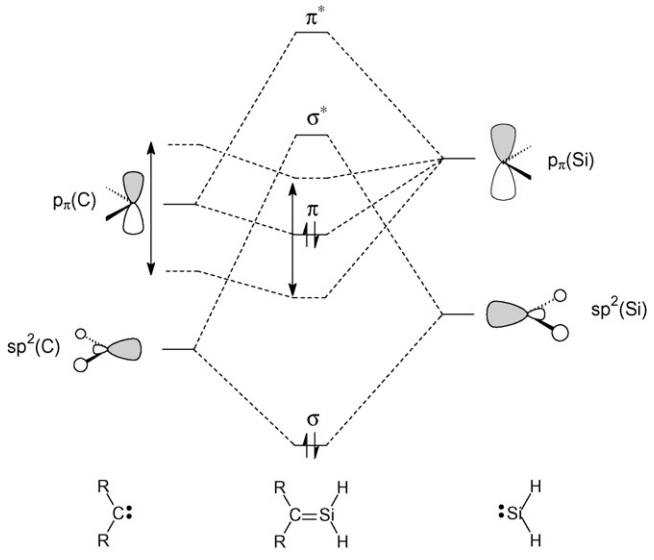

Fig. 5. Orbital interaction diagram displaying the effect of variation in energy of the p_π(C) fragment orbital on the energy of the π MO of an H_2Si=CR_2 silene.

Thus, a series of different qualitative models that describe the bonding in heavy alkenes have been developed. These models can sometimes be linked and used interchangeably to yield the most convenient and transparent analysis.

4. Experimental findings on structure of substituted silenes

Until now, a large collection of experimental information on variously substituted silenes has been gathered. In this section we discuss experimental results that reveal the large effects that substituents can have on the structures of silenes. The section contains illustrative examples and does not represent a complete treatise on all substituted silenes explored thus far.

4.1. Effect of substitution at silicon

In the parent silene the Si=C bond length is 1.7039 Å according to millimeter wave spectroscopy (see Section 2), whereas for 1,1-dimethylsilene (**2**), microwave spectroscopy revealed a Si=C bond length of 1.6921 Å [66], i.e. 0.0118 Å shorter. The finding that Me groups at Si give Si=C bond length reductions agrees with conclusions based on quantum chemical calculations that electron withdrawing groups cause shortenings of the Si=C bond [49–51].

The only silene with dialkyl substitution at Si that has been characterized by X-ray crystallography until now is silene **24** formed by the Wiberg group (Fig. 6) [67]. Silene **24** had a Si=C bond length of 1.702 Å and an essentially planar C_2Si=CSi_2 skeleton, confirming that silenes with dialkyl substituents at Si, and with no π-donor groups at the C-end, have short Si=C bonds. The torsional angle about the Si=C bond was merely 1.6°.

Using the sila-Peterson olefination reaction, Apeloig and coworkers formed silenes with a substitution pattern opposite to that of Wiberg's silene, i.e. silenes with disilyl substitution at Si and dialkyl substitution at C (Scheme 10) [68]. Of these, **25b** and **25c** were stable, and X-ray structural analysis revealed **25b** to have a nearly planar arrangement around the Si=C double bond with a small twist angle of 4.6°. The SiC bond length of 1.741 Å (Fig. 7) was intermediate between that of the parent silene and that of Brook's silene **5a** (*vide infra*). Quantum chemical calculations showed that the Si=C bond elongation was not due to steric congestion, but rather to electronic effects linked to the substitution pattern and thus to the silene polarity [68]. At the MP2/6-31G(d) level, $(H_3Si)_2Si$=CMe_2 (**26**), which serves as a model for **25a**–**25c**, had a Si=C bond length of 1.754 Å. In con-

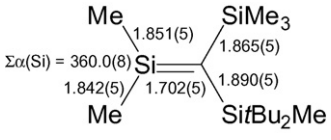

Fig. 6. Selected bond lengths and sum of valence angles at Si ($\sum\alpha$(Si)) of silene **24** determined by X-ray crystallography. Distances in Å and angle in °. Data from Ref. [67].

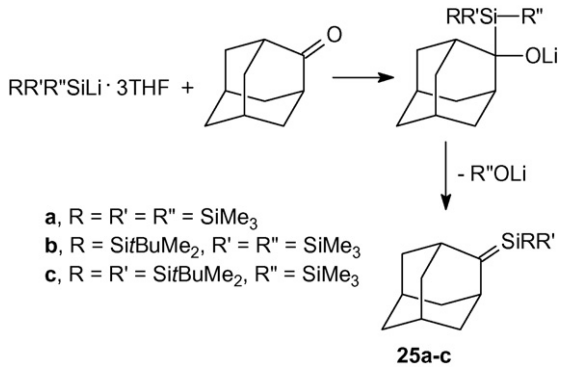

Scheme 10.

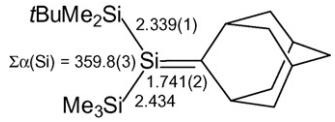

Fig. 7. Selected bond lengths and sum of valence angles at Si ($\sum\alpha$(Si)) of silene **25b** as determined by X-ray crystallography. Distances in Å and angle in °. Data from Ref. [68].

trast, $Me_2Si{=}C(SiH_3)_2$ (**27**), resembling Wiberg's silene **24**, had a shorter computed Si=C bond of 1.722 Å. The calculated Mulliken charges also revealed that **26** is rather nonpolar while **27** is strongly $Si^{\delta+}{=}C^{\delta-}$ polarized.

Very recently, Sekiguchi and co-workers formed the silyl anion substituted silene **28** (Fig. 8) [69]. This species has resemblance to **25**, but has one silyl anionic and one alkoxy substituent at C rather than two silyl substituents. Three possible structural isomers can be drawn (Scheme 11), one being the 1,2-disilaallyl anion **29**. However, delocalization of the negative charge is not as favorable as formation of a Si=C double bond of regular length and localization of the charge to the terminal Si atom. The negative charge at Si1 is localized to an orbital which based on the X-ray crystal structure is orthogonal to the π- and π*-orbitals of the Si=C bond. Moreover, the Si and C atoms of the Si=C bond are essentially sp^2 hybridized and the bond is only modestly twisted.

Indeed, many of the stable silenes that have been investigated experimentally have silyl substituents at Si [1]. The silenes discussed in the next section and that have been characterized by X-ray crystallography, apart from the weak carbene-silylene complex of Boesveld et al. [70], have bulky silyl substituents at Si. Disregarding the small impact on structure caused by

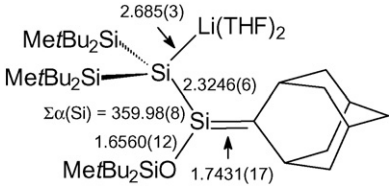

Fig. 8. Selected bond lengths and sum of valence angles at Si ($\sum\alpha$(Si)) of silene **28** as determined by X-ray crystallography. Distances in Å and angle in °. Data from Ref. [69].

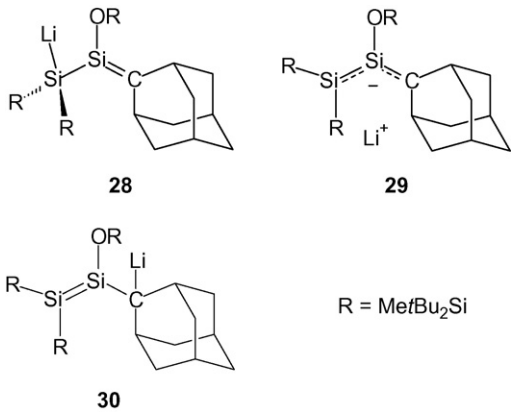

Scheme 11.

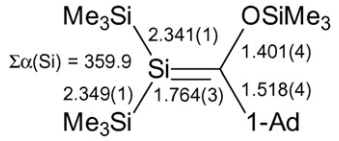

Fig. 9. Selected bond lengths and sum of valence angles at Si ($\sum\alpha$(Si)) of silene **5a** as determined by X-ray crystallography. Distances in Å and angle in °. Data from Ref. [3].

differences in steric bulk of the various silyl groups, the structural impact of the substituents at the C atom can therefore be rationalized.

4.2. Effects of substitution at carbon

The Si=C bond is easily polarized and, as seen in Section 3.3, the largest influence is caused by π-donor substituents at the C atom. Through increased contribution of reverse polarized resonance structure **II** and **III** (Scheme 7), negative charge is donated from the substituent at C to Si reducing the partial positive charge at Si. This elongates the Si=C double bond, as exemplified by Brook's silene **5a** [3]. Above a certain π-donor ability of the substituents at C, pyramidalization of Si also sets in [64].

The X-ray crystal structure of Brook's silene **5a** revealed the Si=C double bond to be 1.764 Å (Fig. 9) [3], much shorter than the normal length of a SiC single bond (1.87–1.91 Å) [71], but longer than that of the parent silene (1.704 Å) [9]. The Si=C bond elongation in **5a** was thus concluded to stem from influence of resonance structure **II** (Scheme 12), and not from steric congestion. The formally sp^2 hybridized Si and C atom were truly planar, but the bond angles involving the two sp^2 hybridized atoms deviated substantially from 120°, presumably a consequence of steric congestion. The molecule was twisted with a

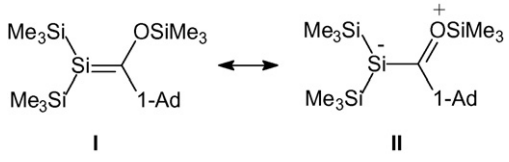

Scheme 12.

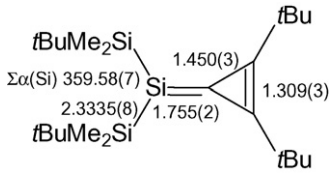

Fig. 10. Selected bond lengths and sum of valence angles at Si ($\sum\alpha$(Si)) of silene **31** as determined by X-ray crystallography. Distances in Å and angle in °. Data from Ref. [58].

twist angle of 14.6°, possibly caused by crystal packing. This may indicate a slightly weakened Si=C π-bond.

Only a few years ago, Kira and co-workers isolated and structurally characterized the 4-silatriafulvene **31** (Fig. 10) [58], that, similar to Brook's silene **5a**, is influenced by reversed Si=C bond polarization through a resonance structure with a positively charged cyclopropenium cationic ring and a negatively charged Si (Scheme 8). In contrast to quantum chemical calculations of smaller 4-silatriafulvenes which indicated a pyramidal Si [57], the X-ray crystal structure of **31** revealed a planar trigonal Si and a Si=C bond length of 1.755 Å. The Si=C bond is thus slightly elongated when compared to that of Apeloig's silene **25b** (1.741 Å) which also has silyl substituents at Si but no π-donor groups at C. It was concluded that crystal packing favors the planar structure in the solid state because solution UV and NMR spectroscopies indicated that at low temperatures **31** adopts a bent structure but as temperature is raised it begins to fluctuate around the planar structure [58].

In silenolates, i.e. Si analogues to enolates (Scheme 13), more negative charge can be placed on Si than in Brook-type silenes and 4-silatriafulvenes. These species have been extensively investigated by the groups of Bravo-Zhivotovskii, Apeloig, Ishikawa, Ohshita, and Ottosson. In 1996, Ishikawa and Ohshita reported the synthesis of four lithium silenolates $(Me_3Si)_2$Si=CROLi with R = Mes (**32a**), *o*-Tol (**32b**), 1-Ad (**32c**), and *t*Bu (**32d**), together with detailed NMR spectroscopic studies of **32a**, **32c** and **32d** [72]. The ^{29}Si NMR spectrum of **32a** indicated that its central Si atom was sp^2 hybridized. Lithium silenolates **32c** and **32d** were less stable than **32a**, but could still be characterized by NMR. Interestingly, NMR spectroscopy indicated that silenolates **32c** and **32d** with alkyl rather than aryl substituents at C had the negative charge more localized to the Si atom, which as a result had more sp^3 character.

By changing the counter ion from Li^+ to K^+, Ottosson and co-workers formed a crystallizable silenolate **33** with *t*Bu substituent at C, and structurally characterized it by X-ray crystallography (Fig. 11) [73]. Silenolate **33** had a SiC bond distance of 1.926 Å, just slightly longer than a regular Si–C single bond, and the Si atom was markedly pyramidal ($\sum\alpha$(Si) = 317.8°). Moreover, the CO bond distance was 1.245 Å, and thus, closer

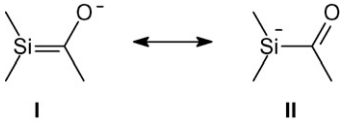

Scheme 13.

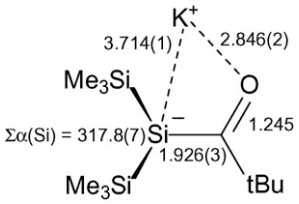

Fig. 11. Selected bond lengths and sum of valence angles at Si ($\sum\alpha$(Si)) of potassium silenolate **33** as determined by X-ray crystallography. Distances in Å and angle in °. Data from Ref. [73].

to that of a C=O double bond than to that of a C–O single bond [74]. Consequently, structural data suggest resonance structure **II** with negative charge at Si to be the most important one (Scheme 13). Even though O is the most electronegative element in the silenolate, ^{29}Si NMR spectroscopy and X-ray crystal structure determination indicated that the Si atom receives the dominant part of the negative charge. The potassium silenolates can thus be designated as acyl substituted silyl anions with only weak Si=C π-bonding.

Very recently, Scheschkewitz and co-workers reported formation of the cyclic silene **34b** (Fig. 12) [75], which bridges the gap between Brook-type silenes and the silenolate reported by Ottosson. Silene **34b** has a tricoordinate Si atom which is somewhat pyramidalized ($\sum\alpha$(Si) = 342.2°), although not to the extent observed in silenolate **33**. The Si=C bond length is only slightly elongated when compared to Brook's silene **5a**. DFT calculations further clarify that the pyramidalization of the Si in **34b** is due to influence of reverse Si=C bond polarization rather than due to bulk of the substituents because the pyramidalization remained in small model compounds of **34b**. Indeed, the temperature dependence of the ^{13}C NMR chemical shifts of the two non-equivalent ipso-C atoms of the tetracoordinate Si-atom of **34b** allowed determination of the $\Delta G^{\ddagger}$ for the inversion of the tricoordinate silene Si atom as 10.3 ± 0.3 kcal/mol.

The tetraamino substituted "silene" **35** of Boesveld et al. is a species with the maximum number of π-donor substituents attached to the formal Si=C double bond (Scheme 14) [70]. Being composed of one benzannulated *N*-heterocyclic carbene and one benzannulated *N*-heterocyclic silylene it bears strong resemblance to the enetetramines formed by the Lemal and Hahn groups [76,77]. However, it had a formal Si=C bond length of 2.165 Å according to X-ray crystallography (Fig. 13), i.e. some 27% longer than of the parent silene (exp. 1.7039 Å [9]). The C atom of the silylene–carbene complex **35** was in a nearly planar environment ($\sum\alpha$(C) = 351.4°), whereas the Si

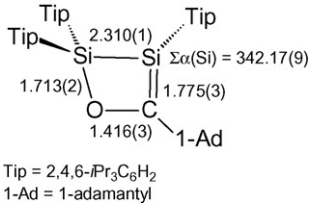

Fig. 12. Selected bond lengths and sum of valence angles at Si ($\sum\alpha$(Si)) of silene **34b** as determined by X-ray crystallography. Distances in Å and angle in °. Data from Ref. [75].

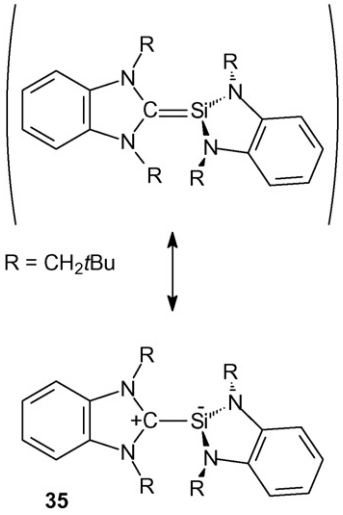

Scheme 14.

atom was strongly pyramidal ($\sum\alpha(\mathrm{Si}) = 291.4^\circ$). Complex **35** was also extensively twisted ($\omega(\mathrm{N–Si–C–N}) = 75^\circ$ and 128°, respectively), indicating complete loss of SiC π-bonding, and the fold angles at C and Si were 28° and 77°, respectively. DFT calculations at the B3LYP/6-311+G(d,p) level on a smaller model compound with R=H instead of CH_2tBu resulted in a structure ($r_{SiC} = 2.204$ Å) that was very similar to that of **35** determined by crystallography, and had an association energy as minute as 3.2 kcal/mol. Indeed, as the temperature was raised, the ^{29}Si and ^{13}C NMR spectra approached those of the free *N*-heterocyclic silylene and carbene, respectively. This species is therefore merely a weak silylene-carbene donor–acceptor complex, and not a silene.

Based on the structural data and DFT calculations, Boesveld et al. concluded that **35** had a $Si^{\delta-}C^{\delta+}$ polar bond, and attributed the dramatic geometric distortions from those of regular Si=C double-bonded compound to reverse polarization [70]. Complex **35** thus exemplifies the very large effect that substituents have on the structures of species that formally can be written as Si=C double-bonded. In an analogous benzannulated enetetramine/tetraaminoalkene **36** (Fig. 14) that has been characterized by X-ray crystallography, the C=C bond length is 1.332 Å [77], well within the range of regular C=C double bonds. Notably, the C–N bond lengths in **36** were longer by ~0.08 Å than those in **35**, indicating a stronger conjugative stabilization of the sp^2 C atom by the amino groups in the latter compound.

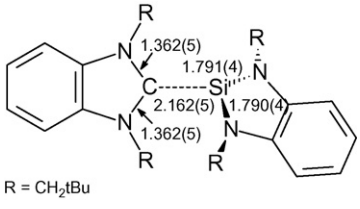

Fig. 13. Selected distances (Å) in the silylene–carbene complex **35** determined by X-ray crystallography. Data from Ref. [70].

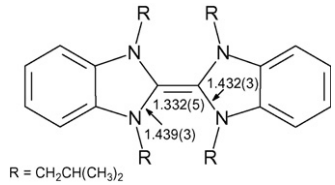

Fig. 14. Selected distances (Å) in enetetramine **36** determined by X-ray crystallography. Data from Ref. [77].

5. π-Bond strengths of substituted silenes

As seen above, the geometry of the silene is markedly influenced by the substituents. The π-bond strength is closely associated with the geometry, and will also be affected by the substituents.

Allison and McMahon used ion cyclotron resonance in conjunction with thermochemical cycles to measure proton and fluoride affinities, and examined the effect of methyl and fluoro substitution at the Si atom on π-bond strength [78]. They found that whereas $Me_2Si{=}CH_2$ (**2**) had a π-bond strength of 39 ± 6 kcal/mol, $FMeSi{=}CH_2$ (**37**) and $F_2Si{=}CH_2$ (**10**) had π-bond strengths of 45 ± 5 and 50 ± 5 kcal/mol, respectively. However, Gusel'nikov and co-workers obtained computational data that showed on an opposite trend [49]. Their conclusions were based on MP4/6-311(d)//MP2/6-31G(d) calculations for $RR'Si{=}CH_2$ species and were determined in two ways: from the calculated enthalpies of dehydrogenation of the corresponding ethylhydrosilanes into the dimethylsilenes, and from extrapolations using frozen equilibrium geometries with R–Si=C–H twist angles up to 60°. This last method was successfully applied by Benassi to determine rotational barriers in alkenes [79]. Both methods showed that the higher the electronegativity of the substituent at Si, the shorter and weaker the Si=C π-bond. For example, according to thermochemical cycles calculated at the MP4 level, **10** had a π-bond energy of 30.9 kcal/mol [49b], i.e. some 20 kcal/mol less than that derived by Allison and McMahon [78]. The Gusel'nikov group also found a good correlation between the π-bond strength and the Pauling electronegativity of the substituents R and R′ of $RR'Si{=}CH_2$ ($r = 0.877$) [49c]. It is noteworthy that Gusel'nikov's findings on the lowered π-bond strength for silenes with electronegative substituents at Si agree with earlier findings for both alkenes and disilenes [80,81].

For silenes that are strongly influenced by reversed Si=C bond polarization, the rotational barrier around the SiC bond will be low because the twisted structure is best described by a closed-shell zwitterionic resonance structure (Scheme 15); the transition state for SiC bond twisting does not involve a singlet biradical transition state. For the $H_2Si{=}C(NH_2)_2$ silene (**19**), Ottosson calculated the SiC rotational barrier to be merely 4.2 kcal/mol at B3LYP/6-31+G(d) level, nearly as low as the rotational barrier for a Si–C single bond which for $H_3Si–CH_3$ is 1.3 kcal/mol at the same level [59,82]. And Boesveld et al. found the rotational barrier of a smaller model of **35** to be only 1 kcal/mol at B3LYP/6-311+G(d,p) level [70].

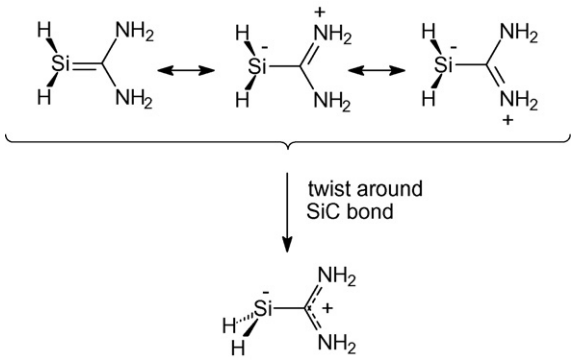

Scheme 15.

Silenolates are also strongly influenced by reverse SiC bond polarization, and on the basis of ^{1}H NMR spectroscopy, the activation energy for rotation about the SiC bond (appr. π-bond energy) in the lithium silenolate **32a** was determined as 14.3 kcal/mol. On the other hand, the ^{1}H, ^{13}C and ^{29}Si NMR spectra of **32c** and **32d** indicated free rotation about the SiC bond, revealing that the sp^{2} character of the central Si atom in these silenolates is lower when compared to that of **32a**.

6. Substituent effects on spectroscopic properties of silenes

Spectral properties are good indicators of the effects that substituents have on the electronic structures of silenes. Table 1 contains NMR spectral data for the silenes that have been isolated so far, with the structures being displayed in Scheme 16. In addition, results from UV–vis, infrared and photoelectron spectroscopic studies will be discussed.

6.1. NMR chemical shifts

The ^{29}Si NMR chemical shift for the 1,1-disilylsubstituted silenes **5a**–**5e** vary in the range of 41–54 ppm (Table 1) [83,84], which is comparable to the ^{29}Si chemical shift of the parent silene (53.8 ppm according to high-level ab initio calculations [15]). This suggests that the Me_3Si group resembles hydrogen when it comes to its effect on ^{29}Si NMR chemical shifts of silenes. When one of the Me_3Si groups was replaced by a *tert*-butyl group (**38a**) the sp^{2}-hybridized Si was deshielded, as can be expected for electronegativity reason, whereas when the Me_3Si group was replaced by a phenyl group, a somewhat smaller downfield shift occurred (**38b**). When the Me_3Si group instead

Table 1
Experimentally determined NMR chemical shifts of a selection of stable silenes

Silene	δ^{29}Si (Si(sp^2)) (ppm)	δ^{13}C (C(sp^2)) (ppm)	Reference
5, $(Me_3Si)_2Si{=}C(OSiMe_3)R$			
5a, R = 1-Ad	41.4	214.2	[83]
5b, R = CEt_3	54.3	207.3	[83]
5c, R = *t*Bu	41.5	212.7	[83]
5d, R = bicyclo[2.2.2]octyl	42.4	212.7	[84]
5e, R = 2-methylcyclohexyl	43.5	212.9	[83]
24, $Me_2Si{=}C(SiMe_3)(SiMe$*t*$Bu_2)$	144.2	77.2	[85]
25, (tBuMe$_2$Si)(RMe$_2$Si)Si=C(2-Ad)			
25b, R = Me	51.7	196.8	[68]
25c, R = *t*Bu	49.7	198.2	[68]
28 $(Me$*t*$Bu_2Si)_2LiSiSi{=}C$(2-Ad)	78.6	130.9	[69]
31,1,2-Di-*tert*-butyl-4,4-bis(*tert*-butyldimethylsilyl)-4-silatriafulvene	−71.9	–	[58]
32, $(Me_3Si)_2Si{=}C(O^-)RLi^+$			
32a, R = 1-Ad	−70.5	–	[72]
32b, R = Mes	−59.9	267.7	[72]
32c, R = *t*Bu	−70.3		[72]
33, $(Me_3Si)_2Si{=}C(O^-)$*t*BuK^+	−78.7	274.1	[73]
34[a]			
34a, R = Tip, R′ = *t*Bu	17.5	213.4	[75]
34b, R = Tip, R′ = 1-Ad	21.9	214.6	[75]
34c, R = SiMe*t*Bu$_2$, R′ = 1-Ad	34.4	231.6	[75]
35[a]	81.9	216.6	[70]
38, $(Me_3Si)RSi{=}C(OSiMe_3)R'$			
38a, R = *t*Bu; R′ = 1-Ad	73.7	195.6	[84]
38b, R = Ph; R′ = CEt_3	61.6	191.2	[84]
39, (Me_3Si)MesSi=C(OSiMe$_3$)1-Ad	41.8	195.8	[86]
40, $Me_2Si{=}C(SiMeROSiMe_3)R'$			
40a, R = *t*Bu; R′ = 1-Ad	126.5	118.1	[84]
40b, R = Ph; R′ = CEt_3	–	110.6	[84]
41[a]	83.5	167.5	[87]
42, $Mes_2Si{=}CHCH_2$*t*Bu	77.6	110.4	[88]

[a] See Scheme 16 for structure.

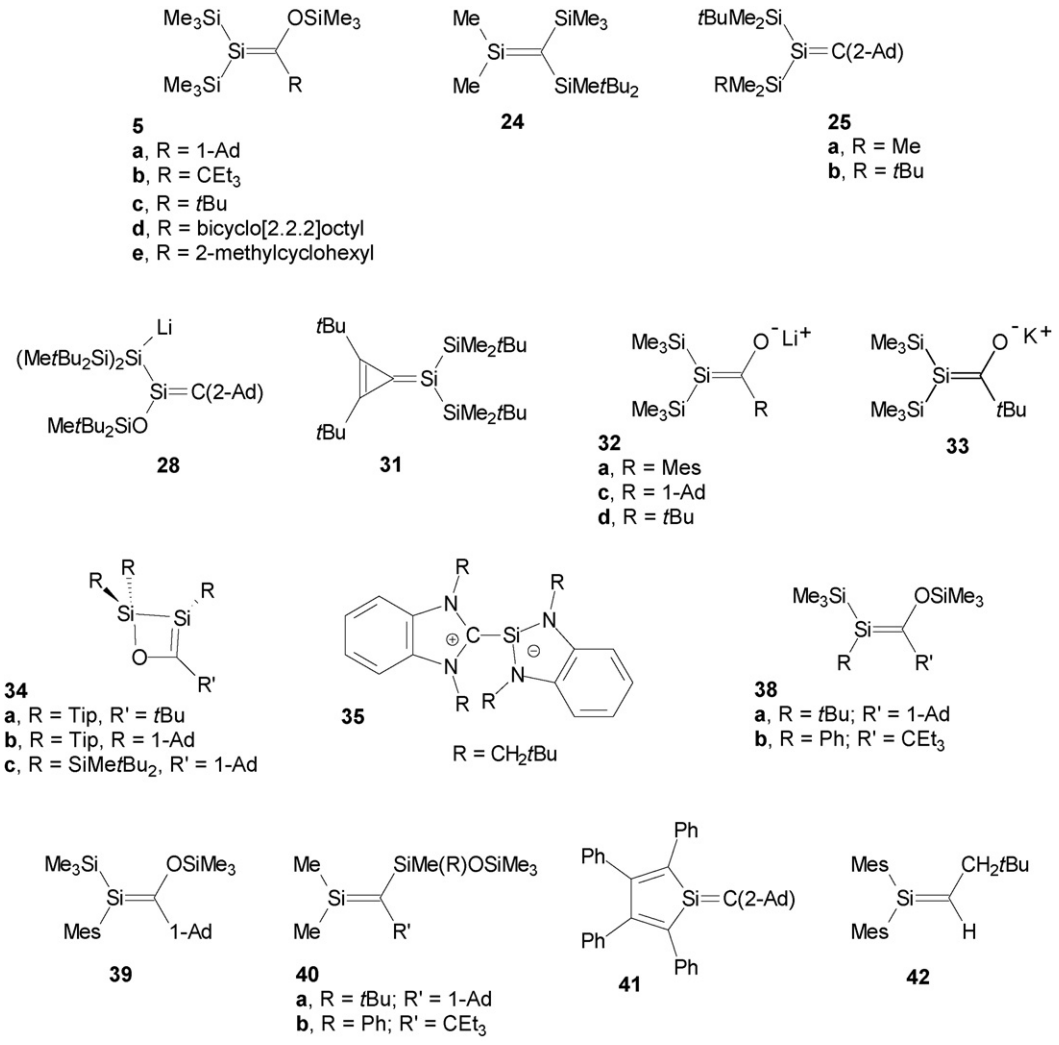

Scheme 16.

was replaced by a mesityl group (**39**), no essential change in ^{29}Si shift compared to **5a** took place. When both Me_3Si groups at Si are replaced by methyl groups as in **24** and **40**, large downfield shifts were found and the ^{29}Si signal appeared in the range 126–145 ppm.

For **31**–**33**, contributions from reverse-polarized resonance structures caused the Si to be significantly shielded (Schemes 8 and 12). The change of the counterion from silenolate **32c** to **33** (Li^+ versus K^+) caused an additional upfield shift of ~8 ppm. However, neither the lithium nor the potassium silenolates had ^{29}Si chemical shift that were as shielded as those of alkyl-*bis*(trimethylsilyl)silyl lithium and potassium compounds (e.g. $Me(Me_3Si)_2SiLi$ and $Me(Me_3Si)_2SiK$ have δ^{29}Si of −133.8 and −127.4 ppm, respectively [89,90]). With regard to silene **41** the influence of reverse polarization is much weaker; instead, this species had a deshielded Si. With two mesityl substituents at Si the stable silene of Couret (**42**) also has π-conjugated substitution at this atom, and its ^{29}Si chemical shift resembles that of **41** [88]. Finally, the ^{29}Si chemical shift of Sekiguchi's **28** appears downfield shifted when compared to Apeloig's **25** a result of the electron withdrawing alkoxy substituent at Si [69].

Even though silene **31** is not equally influenced by reverse Si=C bond polarization as the silenolates **32** and **33**, its ^{29}Si shift of −73.7 ppm appears in the same range. Support for the very upfield shifted ^{29}Si resonance comes from GIAO ab initio NMR chemical shift calculations. The 4-silatriafulvene having the $tBuMe_2Si$ substituents at the Si atom of **31** exchanged to Me_3Si groups (**43**) had a calculated ^{29}Si shift of −68.7 ppm [58]. Interesting temperature-dependent variations in ^{29}Si NMR shifts and UV spectra were also recorded for **31**, and assigned to structural changes from a fluxional planar (room temperature) to a *trans*-bent structure (low temperature). Similarly, the non-planar equilibrium structure of **43** had a calculated ^{29}Si shift of −61.2 ppm. Finally, the Si atom of the weak silylene-carbene complex **35** exhibited a ^{29}Si shift which was moved just slightly more downfield than that of the free silylene (96.9 ppm) [91].

The ^{13}C NMR chemical shifts of the neutral species listed in Table 1 that have Si=C bonds shorter than 1.80 Å appear in the wide range 77–214 ppm. Substituents thus have a dramatic effect also on the δ^{13}C values. For silenes **5a**–**5e**, the ^{13}C chemical shifts of the double bond varied in the narrow range 207–214 ppm, i.e. more downfield from those of regular C=C bonded alkenes (80–150 ppm [16]). Replacing one of the Me_3Si

groups at Si for an alkyl or aryl group (**38** and **39**) caused small upfield shifts of ∼20 ppm.

In **28** the ^{13}C chemical shift comes at 130.9 ppm which is more upfield when compared to silene **25** which has analogous substitution at C. The alkoxy substituent at Si thus increases the $Si^{\delta+}{=}C^{\delta-}$ polarity according to both ^{29}Si and ^{13}C NMR spectroscopy. When both Me_3Si groups are replaced by methyl groups and with one alkyl and one silyl substituents at the C atom, even larger upfield shifts occur so that for **40a** and **40b** the ^{13}C chemical shifts vary in the range 110–118 ppm. And when in silene **24** the second alkyl substituent at C also has been replaced by a silyl group, an even larger upfield shift occurs so that the ^{13}C shift now appears at 77 ppm. Interestingly, the H substituent at C in silene **42** lead to a ^{13}C shift which was similar to that of **40a** and **40b** having one silyl substituent instead.

Two formally Si=C double bonded compounds having SiC bonds longer than 1.80 Å are contained in Table 1. Of these, the silylene–carbene complex **35** had a ^{13}C NMR signal that appeared rather downfield, and it is close to that of the free carbene (231.6 ppm) [70]. For the silenolates, the NMR signal of the C atom was shifted even more downfield, which is expected because of the large influence of the reverse-polarized resonance structure. The difference between lithium and potassium silenolates was only a few ppm with the potassium silenolate displaying the more downfield shifted value.

Both the ^{29}Si and ^{13}C NMR chemical shifts of silenes thus vary widely in dependence of their substitution pattern. Merely permuting positions of alkyl and silyl substituents on the Si=C bond had a large effect [15]. GIAO/B3LYP/6-311+G(2df,p)//B3LYP/6-311+G(2df,p) calculations of $(H_3Si)_2Si{=}CMe_2$ (**26**) and $Me_2Si{=}C(SiH_3)_2$ (**27**) reveal that the ^{29}Si and ^{13}C shifts were 57.2 and 201.9 ppm in the first species, whereas they were 153.9 and 77.2 ppm in the second one.

Finally, the chemical shielding tensors of **25a** and related silenes were examined in a combined experimental and theoretical investigation by West, Apeloig and co-workers [92]. The chemical shift anisotropy (CSA) [93] revealed an interesting dependence on substitution. Silenes **25a** and **26** showed the largest ^{13}C CSA among the silenes studied. This can be related to the substitution pattern which leads to a lower polarity of the Si=C bond and a larger localization of π* and σ* orbitals to the C atom.

6.2. UV–vis absorption spectra

The UV–vis spectra of small silenes either stem from time-resolved absorption spectroscopic studies of transient silenes formed photolytically, or they were recorded for silenes isolated in inert matrices at cryogenic temperatures. The spectra of the sterically protected silenes that are isolable at ambient temperatures were recorded by regular techniques.

The parent silene was characterized by an absorption maximum of the ππ* transition at 258 nm (Table 2) [17], whereas $MeHSi{=}CH_2$ (**44**) and $Me_2Si{=}CH_2$ (**2**) had λ_{max} at 260–265 and 244–255 nm, respectively [94–96]. The attachment of larger alkyl groups at Si, as in **46** and **47** [95], had no noticeable effect on the position of λ_{max} (Table 2). Methyl substitution at C, as in $Me_2Si{=}CHMe$ (**45**) [97], also brought no significant change in λ_{max} compared to $Me_2Si{=}CH_2$. Dichloro substitution at Si causes a modest blueshift as noted when comparing **6** with **49** [98]. Silyl groups, on the other hand, have much larger influence. On the C atom, a redshift of 34 nm was observed when going from $Me_2Si{=}CH_2$ to $Me_2Si{=}C(SiMe_3)_2$ (**53**) [97], and changing the hydrogen at Si in $MeHSi{=}CH_2$ (**44**) to a Me_3Si substituent in $Me(Me_3Si)Si{=}CH_2$ (**50**) caused a redshift in λ_{max} of 20–25 nm [95].

Silenes with substituents that π-conjugate with the Si=C bond showed even more strongly redshifted values for λ_{max} of the lowest ππ* transition. One vinyl or ethynyl substituent at Si (**54** and **55**) gave bathochromic shifts of 47 and 33 nm, respectively [95].

Table 2
UV–vis absorption maxima corresponding to the ππ* transitions of substituted silenes

Silene	λ_{max}	References
6, $H_2Si{=}CH_2$	258	[17]
44, $MeHSi{=}CH_2$	260, 265	[94,95]
2, $Me_2Si{=}CH_2$	244, 255	[95,96]
45, $Me_2Si{=}CHMe$	255	[97]
46, $EtMeSi{=}CH_2$	255	[95]
47, $MetBuSi{=}CH_2$	260	[95]
48, $HClSi{=}CH_2$	255	[96,98]
49, $Cl_2Si{=}CH_2$	246	[98]
50, $Me(Me_3Si)Si{=}CH_2$	285	[95]
51, $Me_2Si{=}CH(SiMe_3)$	265	[97]
52, $Me_2Si{=}CMe(SiMe_3)$	274	[97]
53, $Me_2Si{=}C(SiMe_3)_2$	278	[97]
54, $Me(H_2C{=}CH)Si{=}CH_2$	305	[95]
55, $Me(HC{\equiv}C)Si{=}CH_2$	290	[95]
56a, 1-Silacyclopenta-1,3-diene	296	[99]
56b, 3,4-Dimethyl-1-silacyclopenta-1,3-diene	312	[99]
57a, 1-Silacyclopenta-1,4-diene	270	[99]
57b, 3,4-Dimethyl-1-silacyclopenta-1,4-diene	274	[99]
58, $PhHSi{=}CH_2$	315	[104]
59, $Ph_2Si{=}CH_2$	325	[101]
60, $Ph_2Si{=}CHPh$	398	[100]
61, $Ar(Ar')Si{=}CH_2$		[102]
61a, Ar = 4-MeC_6H_4, Ar′ = 4-MeC_6H_4	325	[102]
61b, Ar = 2-MeC_6H_4, Ar′ = 2-MeC_6H_4	320	[102]
61c, Ar = Ph, Ar′ = 2,6-$Me_2C_6H_4$	315	[102]
61d, Ar = Ph, Ar′ = 2,4,6-$Me_3C_6H_4$	315	[102]
61e, Ar = 2-MeC_6H_4, Ar′ = 2,6-$Me_2C_6H_4$	310	[102]
61f, Ar = 2,6-$Me_2C_6H_4$, Ar′ = 2,6-$Me_2C_6H_4$	295	[102]
5, $(Me_3Si)_2Si{=}C(OSiMe_3)R$		
5a, R = 1-Ad	340	[3b,83]
5b, R = CEt_3	342	[3b,83]
5c, R = *t*Bu	339	[3b,83]
5f, R = Me	330	[103]
25b, (*t*$BuMe_2Si$)(Me_3Si)Si=C(2-Ad)	322	[68]
28[a]	320	[69]
31, 1,2-Di-*tert*-butyl-4,4-bis(*tert*-butyldimethylsilyl)-4-silatriafulvene	352 (298 K) 344 (77 K)	[58]
34[a]		
34a: R = Tip, R′ = *t*Bu	351	[75]
34b: R = Tip, R′ = Ad	355	[75]
34c: R = SiMe*t*Bu_2, Ad	354	[75]

[a] See Scheme 16 for structure.

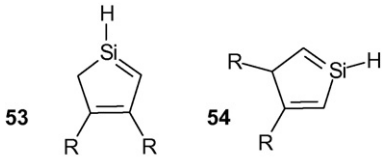

Scheme 17.

From the position of the λ_{max} of the two cyclic silabutadienes **56** and **57** (Scheme 17) it becomes clear that a C=C double bond conjugates better with the Si=C bond when linked to the C atom than to the Si atom [99]. In fact, the larger bathochromic shift of **56** than of **57** compared to $MeHSi{=}CH_2$ has been rationalized by simple Hückel theory [99]. Furthermore, the gradual increase in the number of Ph substituents when going from $H_2Si{=}CH_2$ to $Ph_2Si{=}CHPh$ (**60**) lead to a bathochromic shift of 140 nm [100]. The Ph–Si=C π-conjugation can also be attenuated by twisting the phenyl rings out of the plane of the silene moiety. Increased number of *ortho*-methyl groups bonded to the phenyl substituents of $Ph_2Si{=}CH_2$ (**59**) weakened the conjugation as indicated by a blueshift in λ_{max} of 30 nm when going from **59** to **61a**–**61f** [101,102].

With regard to the larger persistent silenes listed in Table 2, all have λ_{max} values that are significantly redshifted when compared to $H_2Si{=}CH_2$. All of these silenes except one (**28**) have two silyl substituents at Si that will contribute to the observed redshifts. With two silyl groups it is obvious that these shifts should be larger than those given above when going from **44** to **50** (20–25 nm). For silenes **5a**–**5c**, **5f** and **31** [3,58,83,103], the additional redshifts likely stems from conjugation of the Si=C bond with the siloxy substituent or the cyclopropenium system. Interestingly, the smaller Me substituent at the C atom in **5f** when compared to the larger alkyl groups in **5a**–**5c** lead to a blueshift of ∼10 nm [103], presumably a result of less steric congestion in this silene giving a less distorted and stronger Si=C π-bond in this silene. The cyclic silenes **34a**–**34c** which are ring-constrained silenes with some resemblance to Brook-type silenes have λ_{max} at 351–355 nm, i.e. they are further redshifted than the latter ones. The very recently reported silylanion substituted silene **28** has a λ_{max} which is close in wavelength to **25b**.

6.3. IR spectral characteristics

The parent silene $H_2Si{=}CH_2$, the Si-methylated $MeHSi{=}CH_2$, and $Me_2Si{=}CH_2$ have Si=C bond stretch vibrations of 985, 989, and 1003 cm^{-1}, respectively. Thus a Me group at C very modestly blueshifts the Si=C bond stretch [17,94,96,105,106]. Conversely, the attachment of a hydroxyl group at Si, as in $Me(HO)Si{=}CH_2$ (**62**), moves the Si=C stretch vibration to lower wavenumbers (899 cm^{-1}) [107], in accordance with Gusel'nikov's computations that indicate Si=C bond weakening by electronegative substituents at Si [49]. A methyl group at C moves the Si=C bond stretch vibration to slightly lower wavenumbers, as seen when comparing $Me_2Si{=}CH_2$ with $Me_2Si{=}CHMe$ which has a $\nu_{Si=C}$ of 978 cm^{-1} [108]. Even further shifts are seen when the Si=C bond is conjugated with a C=C double bond as in **56a** and **57a** [99]. The vibrations observed at 929 and 936 cm^{-1} in Ar matrices have been assigned to Si=C bond stretches in these two compounds.

With regard to the vibrational transitions in the large stable silenes listed in Table 1, it is more difficult to extract the vibration that predominantly corresponds to the Si=C bond stretch. For **5a**, one could observe bands at 935, 975, and 1005 cm^{-1} by Raman spectroscopy, along with bands at 933 and 1007 cm^{-1} by IR spectroscopy [3b]. Any of these bonds should have a significant portion of Si=C bond stretch vibration.

6.4. Ionization potentials

The ionization potentials of several different silenes have been reported in the literature. Photoelectron spectroscopy performed by Bock and co-workers on the parent silene gave its first ionization potential (IP_1) at 8.9 eV [19]. Several groups investigated $Me_2Si{=}CH_2$ (**2**), and placed its IP_1 in the range 7.5–8.3 eV [109]. For $(Me_3Si)_2Si{=}C(OSiMe_3)$1-Ad (**5a**), Brook and co-workers reported an IP_1 of 7.7 eV [3b].

In 2002, Apeloig and co-workers reported a study that rationalized the experimentally determined IP_1's of $(Me_3Si)_2Si{=}C$(2-Ad) (**25a**), (tBuMe$_2$Si)(Me$_3$Si)Si=C(2-Ad) (**25b**), and a set of smaller silenes [110]. Quantum chemical calculations at the HF, B3LYP, MP4, and OVGF levels were also performed, and the OVGF/6-311+G(2df,p)//B3LYP/6-31G(d) calculations reproduced the experimentally measured IP_1's for the two smallest silenes **2** and **6** contained in the study.

The effect of the substituents on the energy of HOMO (ε_{HOMO}) was assessed [110]. Disilyl substitution at the Si atom of the Si=C bond and dimethyl substitution at the C atom raised ε_{HOMO} by 0.6 and 0.8 eV, respectively. Substitution at the parent silene by four methyl groups (**67**) reduced the IP_1 by 1.5 eV. So far, the ionization potential of **25a** is the lowest measured for a silene, and according to calculations, three factors lead to the low IP_1: dialkyl substitution at C (+0.9 eV), *bis*(trimethylsilyl) substitution at Si (+0.7 eV), and the 2-adamantyl group (+0.4 eV). Indeed, the low IP_1 of **25a** is similar to that of tetrathiafulvalene (TTF) (6.7–6.9 eV) [111], and consequently, silene **25a** also has a low oxidation potential [112], similar to TTF.

Here, it bears to be mentioned that substituted alkenes have a wider span in the IP_1 (10.51–5.95 eV [20,113]) than what is the case for the silenes listed in Table 3. However, the variation in substitution is much greater among the investigated alkenes than among the silenes for which IP's have been measured.

7. Reactivities of silenes in dependence of substitution pattern

In this chapter we discuss the reactivities of differently polarized silenes, even though a fully unambiguous treatment of substituent effects on reactivity is difficult because silenes investigated by different research groups are rarely subjected to the same reaction conditions. We focus on three reaction types,

Table 3
Ionization potentials and negative orbital energies of selected silenes[a]

Silene	IP_1 (exp.)	IP_1 (OVGF)	$-\varepsilon_{HOMO}$ (B3LYP)
$H_2Si{=}CH_2$ (**6**)[b]	8.9	8.72	6.19
$Me_2Si{=}CH_2$ (**2**)[c]	7.5–8.3	7.94	5.46
$(Me_3Si)_2Si{=}C(OSiMe_3)$1-Ad (**5a**)[d]	7.7		
$(Me_3Si)_2Si{=}C$(2-Ad) (**25a**)[e]	6.9		5.02
(tBuMe$_2$Si)(Me$_3$Si)Si=C(2-Ad) (**25b**)[e]	6.9		5.03
$(H_3Si)_2Si{=}CMe_2$ (**26**)[e]		7.71	5.62
$(H_3Si)_2Si{=}CH_2$ (**63**)[e]		8.46	6.21
$(Me_3Si)_2Si{=}CH_2$ (**64**)[e]			5.61
$H_2Si{=}CMe_2$ (**65**)[e]		7.85	5.52
$H_2Si{=}C$(2-Ad) (**66**)[e]			5.40
$Me_2Si{=}CMe_2$ (**67**)[e]		7.18	4.91

[a] Ionization potentials and orbital energies in eV.
[b] From Ref. [19].
[c] From Ref. [109].
[d] From Ref. [3b].
[e] From Ref. [110].

starting with simple dimerization reaction to yield the head-to-tail and/or head-to-head [2 + 2] cycloadducts (Scheme 18). One of the most thoroughly investigated reactions of silenes is that with alcohols, which will be treated next. Finally, the reactions between silenes and several different dienes have been studied. Herein, focus is predominantly on reactions of silenes with 2,3-dimethyl-1,3-butadiene or isoprene.

7.1. Dimerization aptitude

In the absence of other reacting partners, silenes, unless they have very bulky substituents, will dimerize either forming head-to-tail or head-to-head dimers (Scheme 18).

For the parent silene **6**, Venturini et al. used CASPT2 calculations to show that the pathways leading to the two dimers both start with an essentially barrierless ($\Delta E^{\ddagger} = 0.01$ kcal/mol) formation of the 1,4-biradical with a Si–Si bond (Fig. 15) [114]. From this common starting point, the head-to-tail and head-to-head dimers formed through two competitive pathways; the first adduct is formed through a [1,2] silyl sigmatropic shift and the second one through a rotation about the central Si–Si bond in the 1,4-biradical followed by recoupling of the two radicals. The transition states for these two processes have energies of −1.1 and −1.0 kcal/mol relative to two separated $H_2Si{=}CH_2$ molecules. The transition state for the direct formation of the 1,4-biradical having a central Si–C bond, corresponding to the head-to-tail adduct, is at a relative energy of 2.7 kcal/mol. For the parent silene this route will not be competitive, however, substituents may alter the preference in reaction route. The transition state for the [1,2] sigmatropic shift, obtained at the CASPT2/6-311G(d,p)//CASSCF/6-31G(d) level, resembles that earlier reported at the CCSD level of theory by Seidl et al. [115]. The results on 1,3-disilacyclobutane formation from the parent silene are also in accord with observations from matrix isolation studies [17].

Clearly, silenes with bulky substituents are less prone to dimerize, and this is also the case for silenes that are influenced by reversed Si=C bond polarization. An interesting feature is the tendency of various types of substituted silenes toward head-to-tail or head-to-head dimerization. Brook-type silenes, the silenes studied by Apeloig, Ishikawa and Oehme, and possibly also the lithium silenolates of Ishikawa and Apeloig, yield 1,2-disilacyclobutanes [1]. A common theme for all these species is that they have reduced, or even reversed, Si=C bond polarity caused by either π-donor groups at C and/or silyl substitution at Si.

When very bulky substituents are present at the C atom, the head-to-head dimers tend to be thermolabile and can be used for formation of transient silenes (e.g. **25a**, Scheme 19) [116]. Here the bulk of the substituents at C expand the endocyclic C–C bond distance of the 1,2-disilacyclobutane **68** to 1.647 Å, enabling facile cleavage of this bond in the cycloreversion process [117]. In silene **69** (Scheme 20) which has conjugated mesityl substituents at the C atom, Oehme and coworkers postulated involvement of the biradical intermediate **70** in the dimerization process [118]. This biradical intermediate closed to give the observed dimer **71**, which is a formal [4 + 2] cycloadduct between the Si=C bond of one molecule of **69** and the 1-silabutadiene segment involving the Mes group of another **69**. The [4 + 2] adduct decomposed thermally to the 1,2-disilacyclobutane **72**. With even larger aryl substituents such as

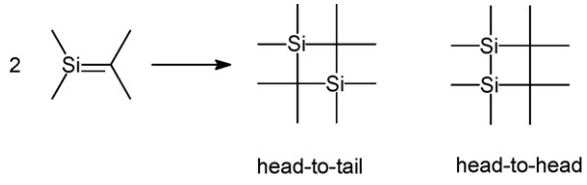

Scheme 18.

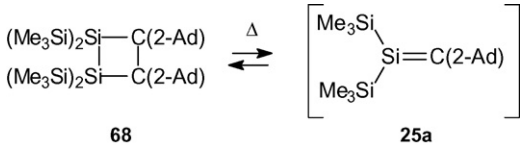

Scheme 19.

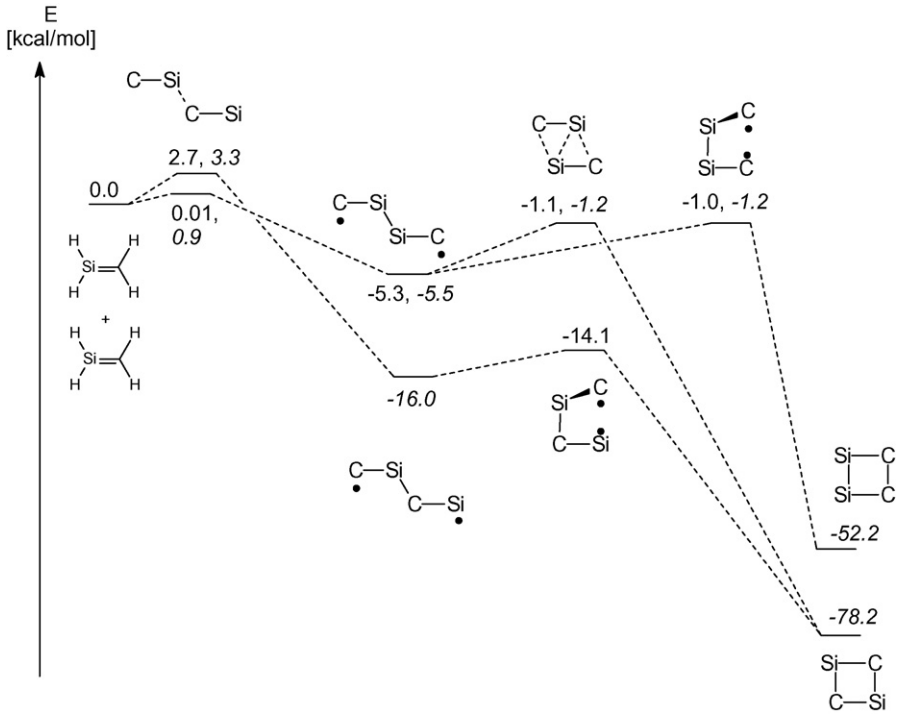

Fig. 15. Relative energies of reactants, transition states, intermediates, and products in dimerization of the parent silene (**6**) at CASPT2/6-311G(d,p)//CASSCF/6-31G(d) (normal print) and CASSCF/6-31G(d) (italics) levels. Values from Ref. [114].

bis(2,4-di-*t*Bu)phenyl and *bis*(2,5-di-*i*Pr)phenyl at C, both the [4 + 2] and [2 + 2] dimers were formed. Finally, EPR spectroscopic investigations of the cycloreversion of the dimers formed from Brook-type silenes indicated involvement of C-centered biradical intermediates; however, no definite assignment was possible [119].

The silyl groups at Si and the siloxy group at C are important for the increased stability of the Brook-type $(Me_3Si)_2Si{=}C(OSiMe_3)R$ silenes **5** [50], yet, the steric bulk of the R group also plays a crucial role in stabilizing these silenes relative to their dimers [3b,120]. The silene (**5c**), with R=*t*Bu, was stable enough to be observed spectroscopically. It was in equilibrium with the dimer **73c**, which had the groups at the ring C atoms in *trans* arrangement (Scheme 21). With the bulkier R=CEt_3 and 1-Ad groups, no silene dimers were formed. A phenyl substituent at the C atom, on the other hand, did not provide the same stabilization as a bulky alkyl group despite the possible conjugative stabilization, and only dimers **73g** were detected [120]. A *p*-methoxyphenyl substituent did not significantly improve the stability of the silene when compared to the phenyl substituent. With a pentafluorophenyl substituent at C, no dimer **73j** was detected, though trapping with methanol

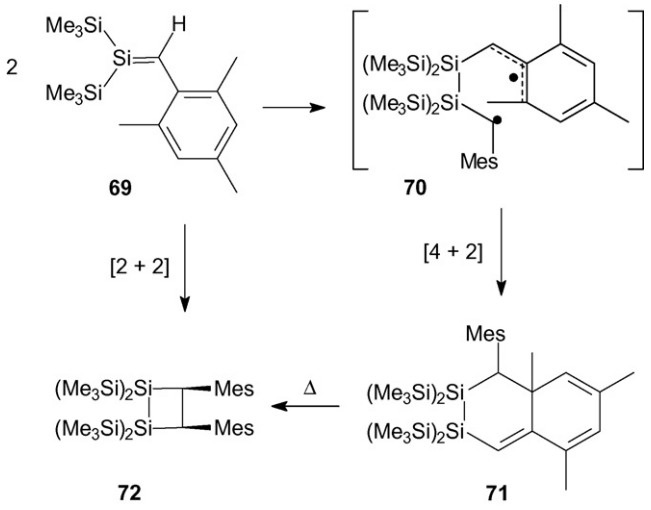

Scheme 20.

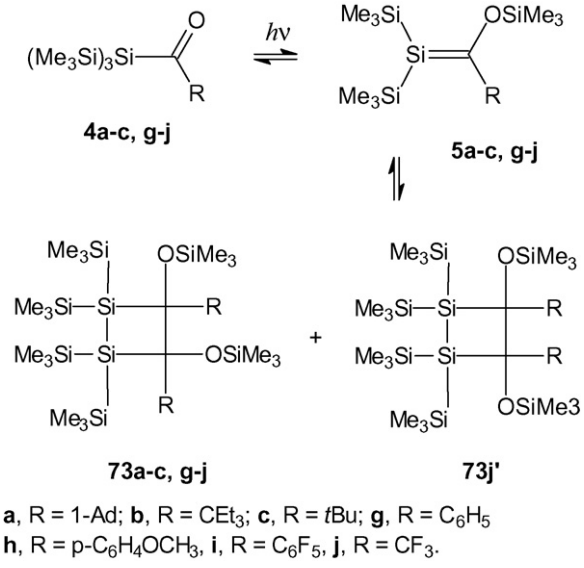

Scheme 21.

indicated that the corresponding silene **5i** was formed [120]. Interestingly, Brook-type silenes with R=CF_3 dimerized to give the *cis*-isomer **73j′** of the 1,2-disilacyclobutane in addition to the *trans*-isomer observed in the dimerization of the other $(Me_3Si)_2Si{=}C(OSiMe_3)R$ silenes [120].

In their 1984 study, Apeloig and Karni analyzed the effects of the substituents on charge distributions as well as energies and coefficients of the π and π* frontier orbitals [50]. Emphasis was given to the factors that govern the kinetic stability of these substituted silenes. The conclusion was that reversed Si=C bond polarity is the single most important electronic factor, and in this regard the energies of the frontier orbitals are not equally important.

Indeed, the Si=C bond polarity has a large effect on dimerization. Using quantum chemical calculations, Ottosson found that the dimerization energy (E_{dim}) decreases dramatically as the influence of reversed Si=C bond polarization increases [64]. Whereas the parent silene (**6**) released 79.3 kcal/mol upon formation of the 1,3-disilacyclobutane, $H_2Si{=}C(NH_2)_2$ (**19**) released only 27.3 kcal/mol in the same process according to B3LYP/6-31+G(d) calculations (Table 4). The E_{dim} for the corresponding 1,2-disilacyclobutane was slightly higher (32.7 kcal/mol). The 4-silatriafulvene (**11**) and 2-hydroxysilene (**17**), which are more moderately influenced by reverse polarization, release 46.4 and 63.6 kcal/mol, respectively, when the 1,3-disilacyclobutanes are formed. Still, the increased thermodynamic stability of silenes that are strongly influenced by reverse polarization may not lead to an increased kinetic stability, even though reduction of the $Si^{\delta+}{=}C^{\delta-}$ bond polarity will lead to lower aptitude for the dipole–dipole complex formation preceding dimerization. However, there is experimental evidence for a reduced dimerization aptitude of reverse polarized silenes. In the thermolytic formation of the transient 2-amino-2-siloxysilenes (**75a**–**75c**, Scheme 22) very little dimer formation was observed [8], and potassium silenolates revealed no tendency for dimerization [73]. Formation of dimers from lithium silenolates was suggested but not proven [72,121].

In contrast, electronegative substituents at Si thermodynamically bias the silene towards head-to-tail dimerization (Table 4). For the series of $RR'Si{=}CH_2$ silenes (R, R′ = H, Me, SiH_3, MeO, NH_2, Cl, F) investigated by Gusel'nikov et al., the cycloreversion enthalpies at MP4 level were in the range 74.1–115.0 kcal/mol [49b], with the largest value calculated for $F_2Si{=}CH_2$ (**10**) (Table 4), i.e. the silene having the highest $Si^{\delta+}{=}C^{\delta-}$ bond polarity.

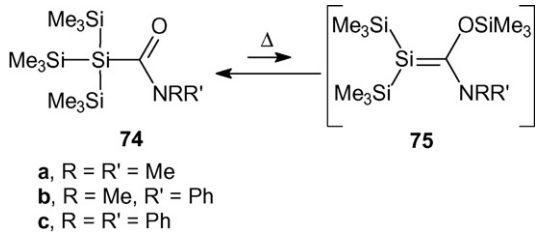

Scheme 22.

Table 4
Energies and enthalpies released upon dimerization of substituted silenes to 1,3-disilacyclobutanes[a]

Silene	E_{dim} (head-to-tail)
$H_2Si{=}CH_2$ (**6**)	79.3, *78.3*
4-Silatriafulvene (**11**)	46.4
$H_2Si{=}CH(OH)$ (**17**)	63.6
$H_2Si{=}CF_2$ (**8**)	68.4
$H_2Si{=}C(OH)_2$ (**20**)	41.4
$H_2Si{=}C(NH_2)_2$ (**19**)	27.3
$(H_3Si)_2Si{=}CH_2$ (**63**)	68.9, *74.1*
$Me_2Si{=}CH_2$ (**2**)	78.4, *85.7*
$(H_2N)_2Si{=}CH_2$ (**76**)	80.5, *88.6*
$F_2Si{=}CH_2$ (**10**)	109.9, *115.0*

[a] Energies in kcal/mol at B3LYP/6-31+G(d) level (normal print) from Ref. [64], and enthalpies at MP4/6-311G(d)//MP2/6-31G(d) level (italics) from Ref. [49b].

7.2. Reactivity towards water and alcohols

Silenes are very electrophilic with the Si atom being the site for attack by water, alcohols, amines, and other nucleophiles. Wiberg and co-workers isolated a THF-silene complex [122], and the attack of alcohols, in particular on naturally polarized silenes, often proceeds in a stepwise manner with the first formation of a similar complex **77** followed by intramolecular proton transfer from O to C (Scheme 23) [15,123,124]. However, investigations by Sakurai revealed that an intermolecular proton transfer can compete with the intramolecular pathway [125], and very recently, Leigh, Bendikov and co-workers revealed yet another mechanism for addition of alcohols to silenes [126]. Silene **25a** was generated photolytically and reacted with methanol. Kinetic data for the addition indicated that the reaction involved the methanol dimer rather than a single methanol molecule. This mechanism was supported by B3LYP and MP2 calculations.

Kira and co-workers were among the first to analyze how the reactivity of silenes towards alcohols and water varies as the polarity of the Si=C bond changes [56,57]. In their experimental investigations they observed a much lower reactivity of the 4-silatriafulvene toward *t*BuOH than for the naturally polarized silenes [56]. They attributed these findings to the reduced

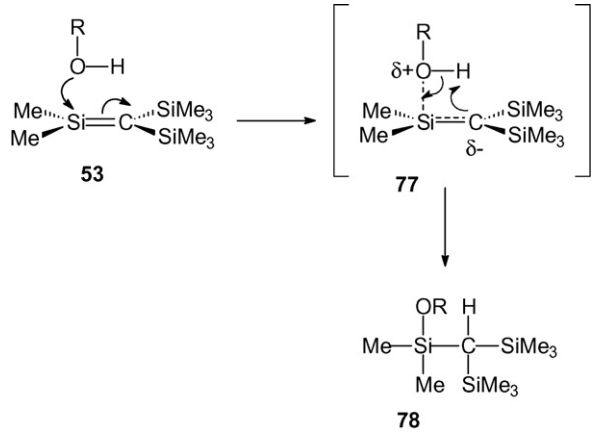

Scheme 23.

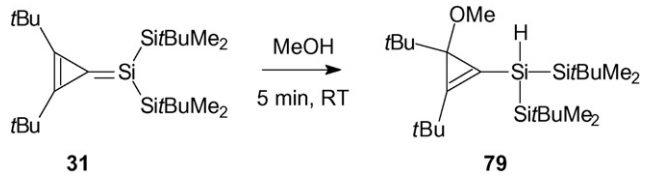

Scheme 24.

polarity of the Si=C bond in 4-silatriafulvene because of the reverse polarized aromatic resonance structure as well as the silyl substituent effect. For the recently isolated 4-silatriafulvene **31** they also observed an abnormal addition of MeOH because the methoxy group added to one of the ring C atoms rather than to the Si atom (Scheme 24) [58].

The Kira group performed MP2/6-311++G(d,p) calculations to analyze the differences in the addition of H_2O to 4-silatriafulvene (**11**) and the parent silene (**6**) [57a] (Fig. 16). The addition of O to Si is the preferred pathway for both silenes. However, whereas the activation energy for the addition of H_2O to **6** is 9.0 kcal/mol, it is 20.0 kcal/mol for **11**, revealing that a lowered positive charge at Si leads to a reduced reactivity towards water. Kira and co-workers further analyzed the activation energies for the abnormal addition of the O atom of water

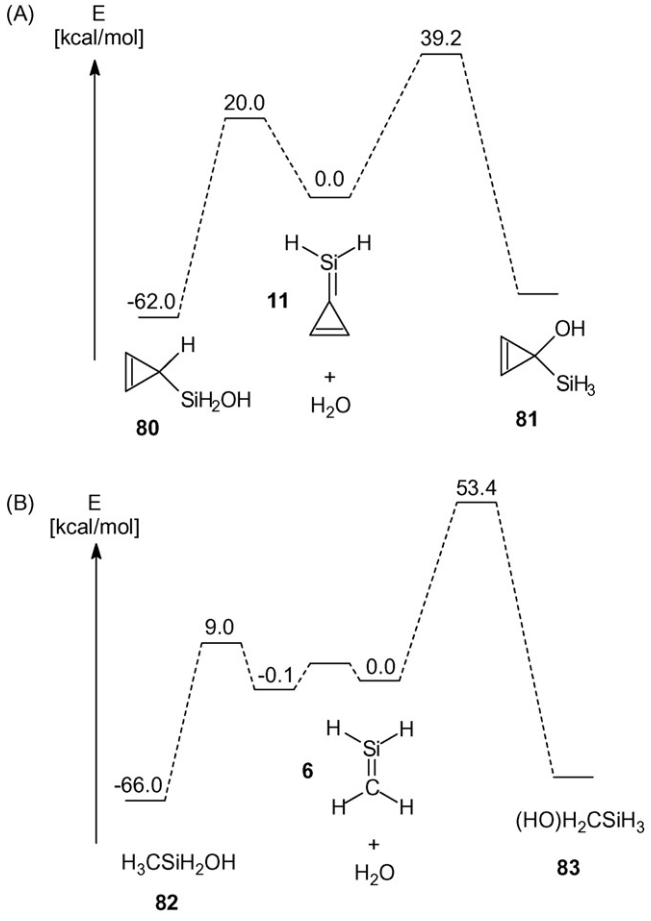

Fig. 16. Energies for reactant, transition states, and normal product in normal and abnormal addition of H_2O to 4-silatriafulvene (A) and the parent silene (B). Energies from MP2/6-311+G(d,p) calculations reported in Ref. [57a].

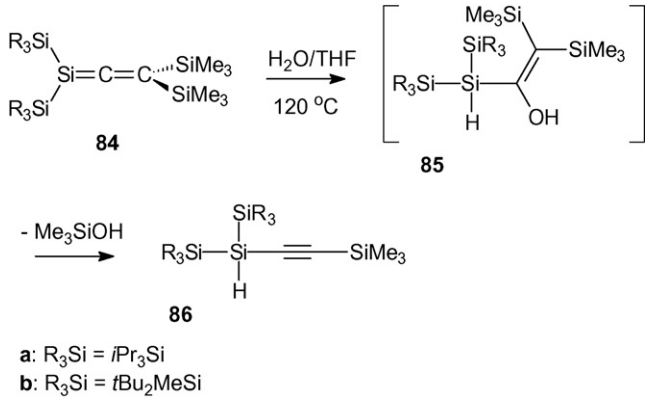

Scheme 25.

to the silene C atom. For both **6** and **11** the activation energies for this type of addition were very high (53.4 and 39.2 kcal/mol, respectively), so this route will not compete with the normal H_2O addition pathway. However, the computational data indicated that the activation energies for H_2O addition to the Si and C atoms of a silene will gradually become more equal as the bond polarity is reduced. In addition to the experimentally observed abnormal addition of MeOH to the ring C atom of Kira's isolable 4-silatriafulvene **31** [58], abnormal H_2O addition to a Si=C bond was also observed by the Sekiguchi group for the persilylated 1-silaallene **84** (Scheme 25) [127], a compound class which is inherently reverse Si=C bond polarized (*vide infra*). Finally, the recently generated cyclic silenes **34a** and **34b**, which also are influenced by reverse polarization, displayed exceptionally high stability; as solid they react only slowly with air and moisture and they do not react with MeOH over a period of 2 weeks [75]. The addition of MeOH must be accelerated with NaOMe and is then completed first within 12 h. Notable is however that the reaction still proceeds by O addition to the tricoordinate Si.

Using laser flash photolysis, Leigh and co-workers have generated over 30 different transient silenes starting from various precursors [128]. Their studies have in particular been directed towards reactions of substituted silenes with various nucleophiles, and they have obtained detailed information about the kinetics and mechanism of the reactions. Herein, we will focus on their investigations of reactions between silenes and alcohols.

A set of transient 1-substituted 1-methylsilenes $RMeSi{=}CH_2$ were generated photolytically from silacyclobutanes and their reactions with methanol, ethanol, and *tert*-butanol were probed (Scheme 26) [95,129]. An acceptable correlation was found between the rate constant for MeOH addition to the $RMeSi{=}CH_2$ silenes and a three-parameter function incorporating resonance, inductive, and steric substituent parameters. This study revealed that the reactivity of the $RMeSi{=}CH_2$ silenes towards MeOH increases with π-donor/σ-acceptor ability of the substituent at Si. On the other hand, the reaction rate was lowered by the steric bulk of the substituents at Si. Thus, silene **55** was the most reactive among the $RMeSi{=}CH_2$, whereas the trimethylsilyl substituent in **50** stabilized this silene relative to that with R = H.

The Leigh group also reported studies on the reactivity of $Me_2Si{=}CRR'$ silenes towards ROH (Scheme 27) [130,131]. A

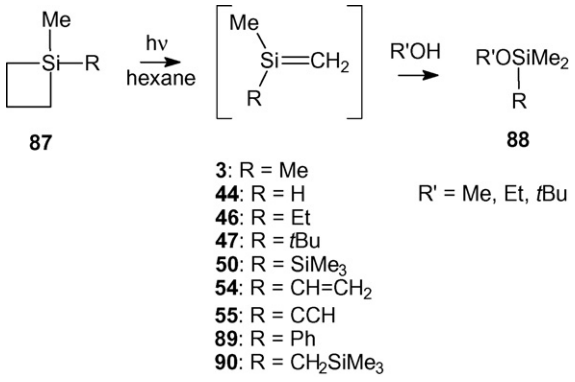

Scheme 26.

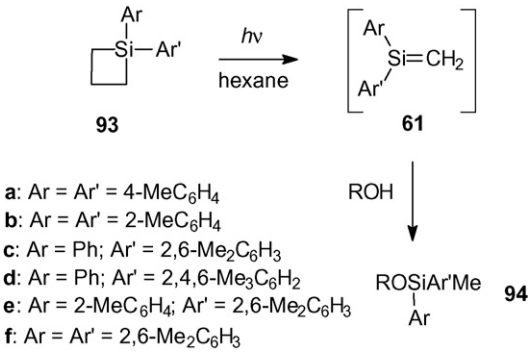

Scheme 28.

comparison with the reactivities of the $RMeSi{=}CH_2$ silenes was made, and the rate constants for the MeOH addition correlated with a function of just one single substituent parameter, the resonance parameter. Including inductive and steric parameters did not improve the fit. Thus, π-electron donor substituents at C stabilize the silenes toward alcohol additions, which supports the previous conclusions that the siloxy substituent in Brook's silene is an important contributor to its lowered reactivity [50]. The principal effect of the π-donor substituents is to decrease the electrophilicity of Si, and thus reduce the rate of formation of a ROH-silene complex.

The $Me_2Si{=}CRR'$ set of silenes investigated by the Leigh group included silene **53** with $R = R' = SiMe_3$ [131]. This species bears strong resemblance to Wiberg's isolable silene **24**, although the latter has a bulkier $SitBu_2Me$ group instead of the $SiMe_3$ group. Silene **53** reacted vigorously with MeOH having the highest reaction rate, and it was concluded that the kinetic stability of Wiberg's isolated silene solely results from the bulk of the $SiMetBu_2$ substituents [131].

In the context of bulk, Leigh and co-workers also studied the combinations of electronic and steric effects on the kinetics and mechanism of addition of methanol, *n*-butylamine, and acetic acid to the 1,1-diarylsilenes **61a–61f** (Scheme 28) [102]. These species had *ortho*-methyl groups on the phenyl substituents at Si. Calculations at the RHF/3-21G* level showed on decreased conjugation between the aryl ring(s) and the Si=C double bond as the number of *ortho*-methyl groups was increased from zero to four. Interestingly, the rate constants for the reaction between the silenes **61a–61f** and the nucleophiles decreased with increased number of *ortho*-methyl groups by as much as a factor of 10,000, indicating that silene reactivity clearly correlates with the bulk of the substituents. Concurrently, the mechanism changed from one that was first-order in ROH concentration (**61b**) to one that was second-order (**61f**).

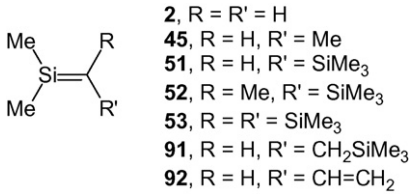

Scheme 27.

The addition of nucleophiles to variously polarized Si=C bonds has also been explored computationally, e.g. by Kira and co-workers as discussed above [57]. More recently, Apeloig and co-workers carried out a systematic study of the potential energy surface for the addition of H_2O, MeOH, EtOH and *t*BuOH to the parent and substituted silenes using ab initio (MP4/6-31+G(d,p)) and DFT (B3LYP/6-31G(d)) calculations [132]. This study included the silenes displayed in Scheme 29.

The effect of the substituents on the charge distribution was very large. The total polarity, Δq, which equals the charge difference between the Si and C atoms increases in the order **96 < 63 < 6 < 50 < 67 < 95 < 49 < 55 < 51**. In all these silenes, the Si atom is the electrophilic site of the Si=C double bond, however, the effect of the substituents on the calculated activation energy $\Delta G^{\ddagger}$ for water addition was large, spanning the range from −3 to 16 kcal/mol. Comparison of the calculated activation energies of silenes **50** and **51** showed that silyl substituents either reduce or enhance the rate of addition, depending on whether these substituents sit at the Si or C atom. Interestingly, the activation barriers for water addition to silenes correlate linearly with the silene polarity Δq. Combining steric bulk with reduced Si=C bond polarity is thus the means for design of novel stable silenes [132].

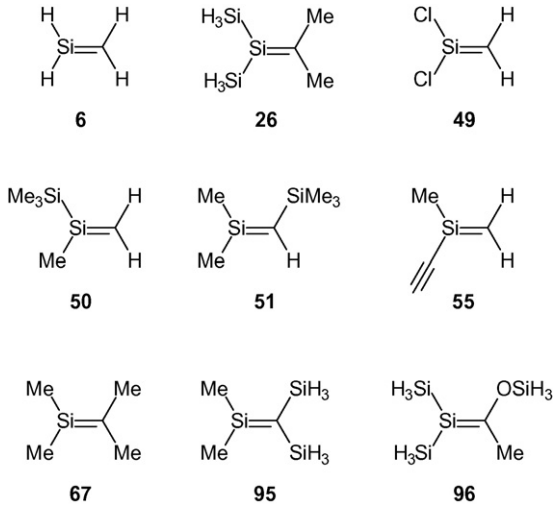

Scheme 29.

7.3. Reactions with dienes

Both [4 + 2] and [2 + 2] cycloadditions, as well as ene reactions, can occur between silenes and dienes, and which of these reaction routes is followed depends to a large extent on the Si=C bond polarity. To enable a proper comparison we focus predominantly on reactions between silenes and either 2,3-dimethyl-1,3-butadiene or isoprene. The latter diene allows discussion of substituent effects on the regioselectivity of the [4 + 2] cycloadditions.

The most strongly naturally polarized silenes are those of Auner, Wiberg, and Couret [1]. The neopentyl silenes of Auner with chloro, alkoxy, or siloxy substituents at Si reacted with 2,3-dimethylbutadiene to give [2 + 2] and ene adducts; no [4 + 2] cycloadducts were formed [133,134]. The 1,1-dichloro substituted silene (**97**) is the most remarkable as 98% of its reaction with 2,3-dimethylbutadiene proceeded via [2 + 2] cycloaddition, yielding the cycloadducts **98** and **99** in similar yields (Scheme 30) [133]. Only 2% gave the ene adduct **100**. The exceptionally high yield of the [2 + 2] cycloadducts was rationalized by frontier molecular orbital theory. According to calculations, silene **97** has a low-lying HOMO, and thus, the $HOMO_{silene}$–$LUMO_{diene}$ energy gap will be larger than for other silenes, leading to a high activation barrier for the concerted [4 + 2] cycloaddition. Interestingly, when either a $SiMe_3$ or phenyl group is attached to the C atom of a 1,1-dichloro-2-neopentylsilene, no [2 + 2] adducts are formed in reactions with 2,3-dimethylbutadiene; only [4 + 2] and ene adducts are observed [135]. Finally, when the substituents at Si in neopentylsilenes were alkyl or aryl groups, predominantly [4 + 2] cycloadducts were formed in reactions with 2,3-dimethylbutadiene [88,136]. With regard to Wiberg-type silenes, they gave both [4 + 2] and ene adducts in reactions with 2,3-dimethylbutadiene [137].

Because of their disilyl substitution at Si, the silenes **25** of Apeloig and co-workers have a lower Si=C bond polarities

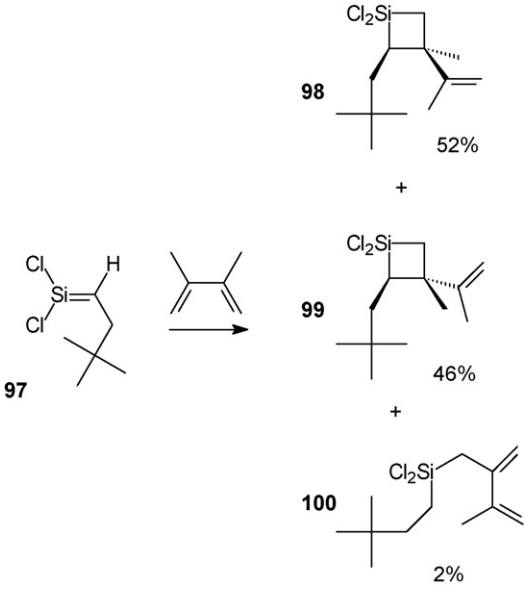

Scheme 30.

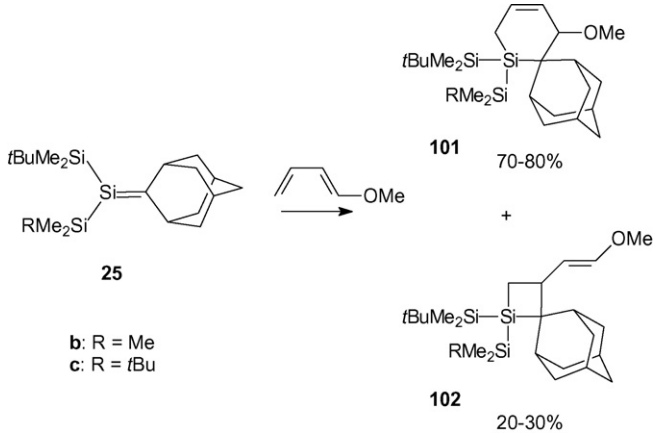

Scheme 31.

than those of Auner, Wiberg, and Couret. In reactions between **25b**–**25c** and 1-methoxybutadiene, the [4 + 2] cycloadducts **101** in 70–80% yield was observed (Scheme 31). The remainder was a single [2 + 2] adduct that resulted from addition of the Si=C bond to the unsubstituted C=C bond of the 1-methoxybutadiene [68]. The [4 + 2] cycloaddition with 1-methoxybutadiene also occurred thermally from the dimer of the less sterically congested $(Me_3Si)_2Si$=C(2-Ad) silene [116].

The $(Me_3Si)_2Si$=C$(OSiMe_3)$R silenes and 4-silatriafulvenes of Brook and Kira, respectively, are moderately influenced by reversed Si=C bond polarity through π-conjugative donor groups at the C atom. The $(Me_3Si)_2Si$=C$(OSiMe_3)$R silenes **5a** and **5c** yielded both [4 + 2] and ene adducts in reactions with 2,3-dimethyl-1,3-butadiene (Scheme 32) [138]. The ratios of [4 + 2]/ene adducts were 1.5:1 for both silenes, and the combined yields were high (>98% based on NMR). Similar product ratios were noted when the reactions were carried out in the dark with preformed silene and when the silene was formed photolytically in presence of diene. In contrast, [2 + 2] cycloadducts were found in higher yields than the [4 + 2] cycloadducts in reactions between $(Me_3Si)_2Si$=C$(OSiMe_3)$R silenes and 1,3-butadiene [138]. When the 4-silatriafulvene **106** was formed from the anthracene adduct **105** (Scheme 33), it reacted exclusively in [4 + 2] manner with 2,3-dimethylbutadiene in very high yield [56].

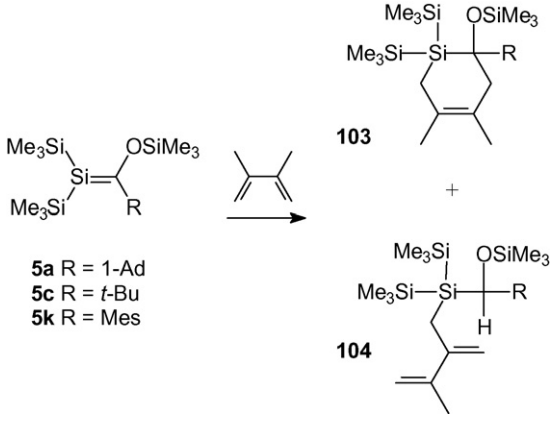

Scheme 32.

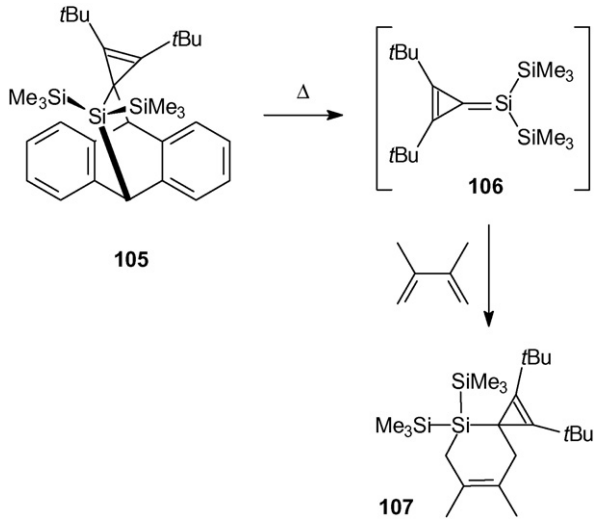

Scheme 33.

Ottosson and co-workers formed more strongly reverse polarized silenes, 2-amino-2-siloxysilenes (**75**), as transient species through thermolysis of carbamylsilanes, and trapped these silenes with 2,3-dimethylbutadiene (Scheme 34) [8]. Formation of the same silenes without presence of trapping reagent was earlier attempted photolytically by Lickiss, Brook and co-workers, however, without reported success [139]. When generated thermally and trapped with dienes a single [4 + 2] cycloadduct **108** was formed in nearly quantitative yields, and it resulted from a [4 + 2] cycloaddition followed by an anomerically assisted migration of $OSiMe_3$ and $SiMe_3$ groups in the initially formed cycloadduct. Finally, lithium and potassium silenolates are species that are nearly completely described by the reverse polarized resonance structure with the negative charge at Si (Scheme 13). Ohshita and co-workers found that the lithium silenolates **31** gave exclusively [4 + 2] cycloadducts with 2,3-dimethylbutadiene (Scheme 35) [140].

The polarity of the Si=C bond seems to be key to the regiochemistry of [4 + 2] cycloadditions between silenes and isoprene. The reactions between Wiberg's naturally polarized

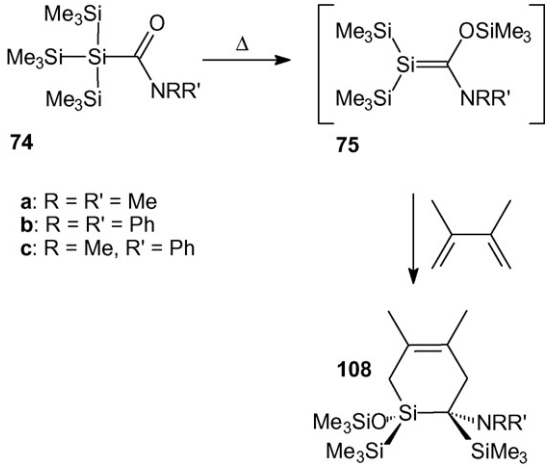

Scheme 34.

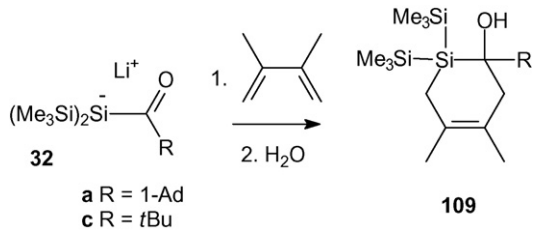

Scheme 35.

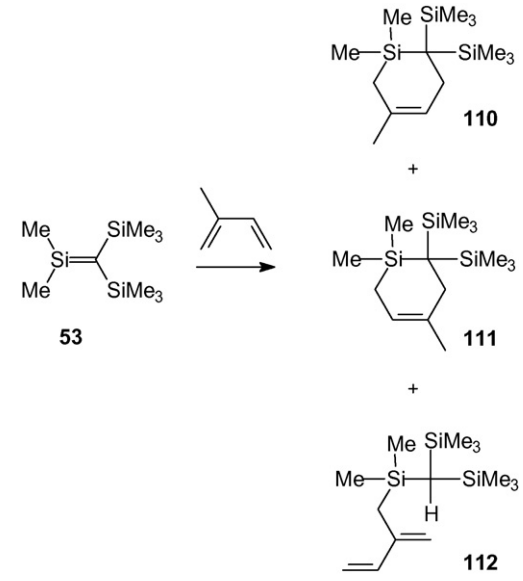

Scheme 36.

$Me_2Si{=}C(SiMe_3)_2$ silene (**53**) and isoprene gave the two silacyclohexenes **110** and **111** in a 66:8 ratio (Scheme 36) [141]. For reactions with Brook-type silenes, the isomeric silacyclohexenes **113** and **114** were obtained in a ratio of 1:3 [138], and constituted 89% of the total yield (Scheme 37). When a

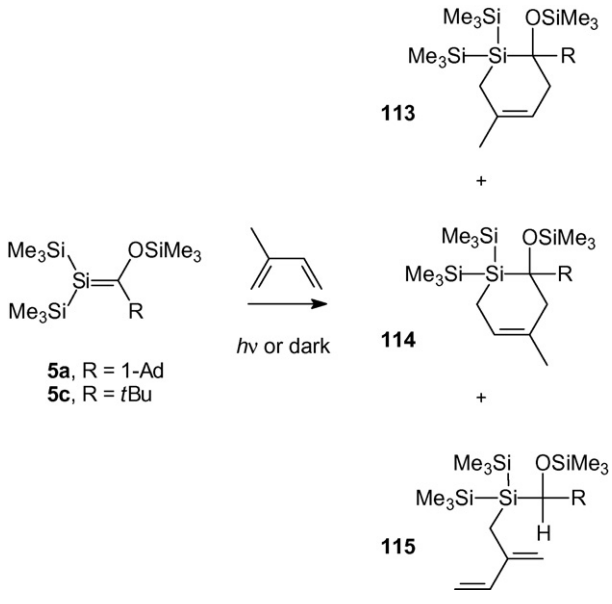

Scheme 37.

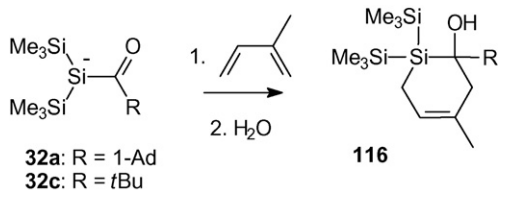

Scheme 38.

lithium silenolate was reacted with isoprene, only regioisomer **116** shown in Scheme 38 was detected [140].

An interesting feature is the predominant formation of the "meta" versus "para" product in reactions between isoprene and the variously polarized silenes. The major "meta" product **110** formed in Wiberg's study could have stemmed from the significant $Si^{\delta+}=C^{\delta-}$ polarization of this silene reacting to maximize frontier orbital interactions with the slightly polarized isoprene. The opposite regiochemistry in the reactions of the Brook-type silenes with isoprene was considered to originate from both steric hindrance in the transition states leading to the two products, as well as to frontier orbital interactions because the preference for the "para" product in reactions of Brook-type silenes could be explained by the large coefficients of both HOMO and LUMO on Si [138]. The lithium silenolates are even more reverse polarized than Brook's silenes, and now the regiochemistry of the [4 + 2] cycloaddition between these substrates and isoprene was completely in favor of the "para" product **116** (Scheme 38) [140].

8. The Si=C bond in allenic structures: effect of heteroatom substitution

The Si=C bond can also be included in allenic structures, although only allenes with Si at the terminal site have been synthesized as isolable species. These species are related to substituted silenes because both the Si=C bond length and the structure around Si depend strongly on the atom at the opposite end as well as on the substituents at Si. Herein, we focus on the allenic compounds Si=C=X with $X = CR_2$, NR, and O. To predict the bonding in these compounds using CGMT theory one needs to regard the ΔE_{ST} of $C{=}CH_2$, C=NH, and CO. These species all have singlet ground states and their ΔE_{ST} at the B3LYP/6-311+G(d,p) level are 47.5 ($C{=}CH_2$), 104.7 (C=NH), and 134.8 (CO) kcal/mol [59]. Similar gaps for $C{=}CH_2$ and CO were reported by Trinquier and Malrieu (46 and 139 kcal/mol, respectively) [29]. Based on CGMT theory, one can predict a successively more nonclassical structure upon moving from 1-silaallenes via 1-silaketeneimines to 1-silaketenes [29].

8.1. 1-Silaallenes

In 1993, West and co-workers formed the first stable and isolable silaallene **117** (Scheme 39) [142]. This species is still among the least reactive Si=C bonded compounds prepared; it can be handled in the presence of air and water under nonacidic conditions for several days. Its stability is due to both the extreme bulk of substituents and an inherent electronic stabilization of

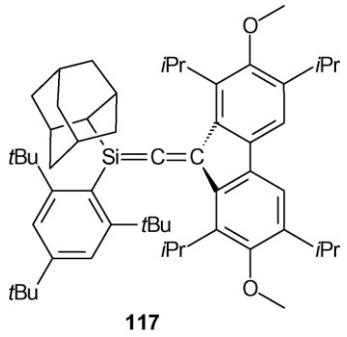

Scheme 39.

silaallenes. The Si=C and C=C bond lengths of **117**, as measured by X-ray crystallography, were 1.704 and 1.324 Å, respectively, the Si=C=C bond angle was 173.5°, and the geometry around the Si atom was planar. Even though the Si=C bond length of **117** agreed closely with that of Wiberg's silene **24** (1.704 Å) [67], the ^{29}Si and ^{13}C NMR chemical shifts of 48.4 and 225.7 ppm of **117** suggested that its Si=C bond is much less polar. Instead, the NMR chemical shifts were similar to those of Brook's silene **5a** ($\delta^{29}Si = 41.4$ ppm and $\delta^{13}C = 214.2$ ppm), and it was concluded that 1-silaallenes exhibit a partial reversed polarity of the Si=C bond. Earlier quantum chemical calculations [50,143], suggested that the extent of the reverse polarization effect is comparable to that found for a Si=C bond having a π-donating substituent at C, but without the bond elongation [142].

A few years later, three additional 1-silaallenes, **118a**–**118c** (Scheme 40), were reported by the West group [144]. The length of the Si=C bond in **118a** was as short as 1.693 Å. Again, the Si=C=C bond angle was somewhat bent (172.0°), and now the Si atom was slightly pyramidal ($\sum\alpha(Si) = 357.2°$), whereas the terminal C atom was essentially planar. 1-Silaallene **118a** was rather unreactive toward oxygen, but reacted instantly with water and methanol to nearly quantitatively give either hydroxyvinylsilane or methoxyvinylsilane. In these reactions the O atom added to Si, in accord with a natural Si=C bond polarity.

With two aryl substituents at Si, **118a** has a ^{29}Si NMR chemical shift of 13.1 ppm, i.e. even more shielded Si than that of **117**. Changing the two tri-*iso*-propylphenyl (Tip) substituents to one *t*Bu and one tri-*tert*-butylphenyl substituent (Mes*) at Si, leading to **118b** and **118c**, caused the ^{29}Si shift to move to 55.1 (for **118b**) and 58.7 ppm (for **118c**). Clearly, the substituents at Si influence the charge distribution of the Si=C bond of 1-silaallenes as they do for silenes.

Whereas the 1-silaallenes of West had aryl and alkyl substituents, Sekiguchi and co-workers synthesized two persilylated 1-silaallenes, **84a** and **84b**, which appeared as long-lived but

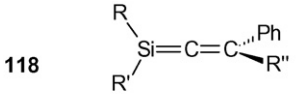

a: R = R' = 2,4,6-tri-iso-propylphenyl (Tip), R'' = *t*Bu
b: R = 2,4,6-tri-tert-butylphenyl (Mes*), R' = R'' = *t*Bu
c: R = 2,4,6-tri-tert-butylphenyl (Mes*), R' = *t*Bu, R'' = Ph

Scheme 40.

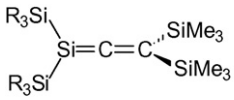

84
a: $R_3Si = iPr_3Si$
b: $R_3Si = tBu_2MeSi$

Scheme 41.

photolabile reaction intermediates (Scheme 41) [127]. Unfortunately, they could not be separated from the reaction mixture, but as judged from the ^{29}Si and ^{13}C NMR data indicated that their Si=C bonds were even more reverse polarized than those in West's 1-silaallenes. The ^{13}C shift of 268.3 ppm revealed a very deshielded central C atom, and the ^{29}Si shift of −64.5 ppm for the central Si atom indicated that is was very shielded. This ^{29}Si shift is similar to that of Kira's 4-silatriafulvene (−71.9 ppm [58]) and those of the silenolates prepared by Ohshita, Ishikawa, and Ottosson (−79 to −60 ppm [72,73]).

Sekiguchi's 1-silaallenes **84** also displayed interesting reactivity toward water as the O atom added to the C atom of the Si=C bond instead of to the Si atom (Scheme 25) [127]. 1-Silaallenes **84** were also relatively stable towards moisture. Their stability and abnormal hydration reactivity presumably stem from the electron-donating effect of the trialkylsilyl groups on the terminal Si atom, in addition to the inherent reverse polarized charge distribution of the 1-silaallene skeleton. As a consequence, its reactivity is similar to that of Kira's isolated 4-silatriafulvene, for which the O atom of methanol added to a C atom of the cyclopropenium ring rather than to Si [58].

Sigal and Apeloig recently examined substituted 1-silaallenes using quantum chemical calculations (Scheme 42) [145]. 1,1-Disubstituted 1-silaallenes with either Me (**119**), SiH_3 (**120**), or F (**121**) substituents were compared to the parent species (**122**), and of these only the 1,1-difluoro substituted species had a pyramidal Si with $\sum\alpha(Si) = 332.5°$ at the B3LYP/SDD level. This species also had a significantly longer Si=C bond (1.788 Å) than the other three (1.712–1.724 Å), and its SiCC angle was markedly bent (147.1°). The energy needed for planarization of **121** was calculated as 6.0 kcal/mol. Whereas Gusel'nikov et al. earlier found $F_2Si{=}CH_2$ to be close to the breakpoint at which nonplanarity sets in according to CGMT theory ($\sum\Delta E_{ST} \geq 1/2E_{\sigma+p}$) [49], $F_2Si{=}C{=}CH_2$ is past this breakpoint because the ΔE_{ST} of $C{=}CH_2$ is positive and large (47.5 kcal/mol with B3LYP/6-311+G(d,p)). This is in contrast to that of CH_2 which even has a triplet ground state ($\Delta E_{ST} = -12.2$ kcal/mol with B3LYP/6-311+G(d,p)). The nonplanarity of **121** is thus in accord with CGMT theory.

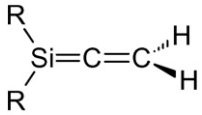

119: R = Me
120: R = SiH_3
121: R = F
122: R = H

Scheme 42.

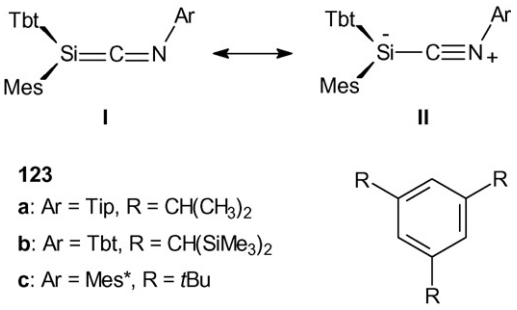

Scheme 43.

8.2. 1-Silaketeneimines

In 1997, Tokitoh and co-workers synthesized the first isolable silaketenimines, **123a–123c**, and concluded that they were best characterized as silylene–isocyanide complexes rather than silaketenimines [146]. None of these three species could be crystallized, however, a B3LYP/6-31G(d) calculation of $Ph_2Si{=}C{=}NPh$ (**124**) revealed a Si–C distance of 1.882 Å, a CN distance of 1.180 Å, and a $\sum\alpha(Si)$ of 306.8°. This demonstrated the silylene/Lewis base character of this compound, which has electron density donated to the Si (Scheme 43). The ^{29}Si NMR chemical shifts were in the range −57.4 to −48.6 ppm, indicating a reverse polarized SiC bond and that the zwitterionic resonance structure **II** dominates.

Very recently, Kira and co-workers reported the synthesis and structure of the silaketenimines **125a** and **125b** (Scheme 44), which in contrast to **123** had stronger allenic character [147]. This is strong evidence that the structures of silaketenimines vary extensively depending on the substituents. Both **125a** and **125b** were stable in the solid state below 0 °C, but dissociated to the silylene and the corresponding isocyanide in solution even at low temperatures. Their Si=C bond lengths according to X-ray crystallography were 1.794 and 1.782 Å, respectively, nearly perfectly in the middle between a Si=C double and a Si–C single bond length. Moreover, the C–N distances of 1.203 (**125a**) and 1.210 Å (**125b**) were significantly longer than the corresponding distances in arylisocyanides (approximately 1.160 Å) [148], indicating a bond order lower than three. The N atom was sp^2 hybridized in both **125a** and **125b**, and although the Si atom was strongly pyramidal in both cases ($\sum\alpha(Si) = 330.6°$ in **125a** and

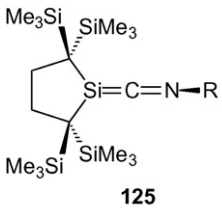

125
a: R = Dip;
b: R = 1-Ad

Scheme 44.

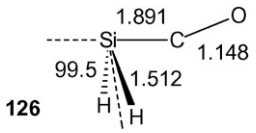

Fig. 17. Optimal geometry of $H_2Si{=}C{=}O$ (**126**) at B3LYP/6-31G(d,p) level. Distances in Å and angles in °. Values from Ref. [149].

331.2° in **125b**), it was not as pyramidal as the Si atom of **124** ($\sum\alpha(Si) = 306.8°$).

The bonding characteristic of 1-silaketenimines is thus sensitive to the substituents, and B3LYP/6-31+G(d,p) calculations showed that (*N*-aryl)diarylsilaketenimines were zwitterionic, (*N*-alkyl)dialkylsilaketenimines were allenic, and (*N*-aryl)dialkyl derivatives could be allenic or zwitterionic, depending on how the *N*-aryl ring is oriented relative the nitrogen lone pair.

8.3. Silaketenes

Carbon monoxide has a large ΔE_{ST} (137 kcal/mol at the B3LYP/6-311+G(d,p) level [59]), and based on CGMT theory one can thus predict that silaketenes will have the most nonplanar structures of the Si=C=X allenes discussed here. Indeed, this is the case. Maier et al. generated the parent silaketene $H_2Si{=}C{=}O$ (**126**, Fig. 17) under cryogenic conditions [149], and using IR spectroscopy determined its structure through correlation of the measured IR spectrum with those calculated at B3LYP level for a series of compounds isomeric to **126**. Silaketene **126** is just a weak donor-acceptor complex between H_2Si and CO with a coordination energy of 23.4 kcal/mol at B3LYP/6-311+G(d,p) level and 21.5 kcal/mol at the MP2/6-31G(d) level. The comparison of computed and measured IR spectra revealed that the Si in H_2SiCO is strongly pyramidal, and the calculated $\sum\alpha(Si)$ was 277.3°. The SiC distance corresponded to a Si–C single bond, and the CO distance was close to that calculated for carbon monoxide (1.138 Å at B3LYP/6-31G(d,p) level).

In addition to the parent silaketene, the $Me_2Si{=}C{=}O$ (**127**) and $MePhSi{=}C{=}O$ (**128**) silaketenes have been reported from matrix isolation spectroscopic studies [150,151]. The B3LYP/6-311++G(2d,p) optimized geometry of **128** was very similar to that of **126**, whereas the calculated coordination energy between MePhSi and CO is merely 11.5 kcal/mol, approximately half that of **126**.

Finally, as CO is isolelectronic with N_2 it is noteworthy that UV–vis absorption spectroscopy of $SiMe_2$ in Ar and N_2 matrices at cryogenic temperatures ($\lambda_{max} = 480$ nm in an Ar matrix and 330 nm in an N_2 matrix [152]) indicates that this silylene also forms weak donor–acceptor complexes with N_2 as a significant shift in λ_{max} occurs in this matrix. However, as N_2 has an even higher ΔE_{ST} than CO (161.3 kcal/mol versus 134.8 kcal/mol at B3LYP/6-311+G(d,p) level [59]), the Me_2SiNN complex should be extremely weakly bonded according to CGMT theory.

9. Concluding remarks

Several qualitative models have been developed to describe the bonding in heavy alkenes, including silenes. The model of Carter, Goddard, Malrieu, and Trinquier (CGMT), which relates the sum of the singlet–triplet energy gaps of the interacting carbene and silylene fragments of a substituted silene ($\sum\Delta E_{ST}$) to the total $\sigma + \pi$ bond energy ($E_{\sigma+\pi}$), has proven particularly useful. In an approximate sense, it can be used to explain why a particular substituted silene has a more pronounced nonclassical structure than another. The strength of the second-order Jahn–Teller (SOJT) distortions is also influenced by substitution because electronegative substituents reduce the gap between π and σ^*, thereby enabling a stronger mixing of these two orbitals when leaving the highly symmetric planar geometry.

The structures of formally Si=C double-bonded compounds vary between those with regular covalent $\sigma + \pi$ bonds, and those that are better described as weak donor-acceptor complexes. Clearly, the nature of the substituents has a larger impact on silenes than on alkenes. As a result, silenes can have classical planar structures in analogy with alkenes, but with sufficiently strong π-electron donor substituents the silene will have a nonclassical nonplanar structure. In the limit, it is a very weak donor–acceptor complex that equilibrates with a separated silylene and carbene.

The electron distribution in the Si=C double bond is easily polarized, and depending on the substituents, silenes can be naturally ($Si^{\delta+}{=}C^{\delta-}$) polarized or reverse ($Si^{\delta-}{=}C^{\delta+}$) polarized. NMR chemical shifts reflect this polarization because the ^{29}Si shift can vary between −79 and 144 ppm, and the ^{13}C shift varies between 77 and 274 ppm, which is larger than the span for alkenes.

Reactions with water and alcohols are indicators of the polarity of a silene. Naturally polarized silenes add water/alcohol to the Si atom, whereas a persilylated 1-silaallenes and a 4,4-disilylated 4-silatriafulvene, which both are influenced by reverse Si=C bond polarization, add water/MeOH at C atoms. Silenes influenced by reverse polarization also tend to react with dienes exclusively in [4 + 2] manner, whereas some strongly naturally polarized silenes give exclusively [2 + 2] cycloadducts.

The data on substituted silenes gathered in the past years thus indicate that the properties of silenes can be tuned widely, and rather predictively, by the choice of the substituents. We hope that this collected knowledge will be particularly valuable in developing potential applications of Si=C bonded compounds in a range of areas spanning from target-directed organic synthesis to materials science.

Acknowledgement

The authors are grateful to the Swedish Research Council for financial support.

References

[1] (a) For general reviews about silenes, see e.g.: A.G. Brook, M.A. Brook, Adv. Organomet. Chem. 39 (1996) 71;
(b) T. Müller, W. Ziche, N. Auner, in: Z. Rappoport, Y. Apeloig (Eds.), The Chemistry of Organic Silicon Compounds, vol. 2, John Wiley & Sons Ltd., New York, 1998, pp. 1233–1310;
(c) R. West, J. Organomet. Chem. 21 (2001) 467;
(d) L.E. Gusel'nikov, Coord. Chem. Rev. 244 (2003) 149.

[2] L.E. Gusel'nikov, M.C. Flowers, J. Chem. Soc. Chem. Commun. (1967) 864.
[3] (a) A.G. Brook, F. Abdesaken, B. Gutekunst, G. Gutekunst, R.K. Kallury, J. Chem. Soc. Chem. Commun. (1981) 191;
(b) A.G. Brook, S.C. Nyburg, F. Abdesaken, B. Gutekunst, G. Gutekunst, R.K.M. Kallury, Y.C. Poon, Y.M. Chang, W. Wong-Ng, J. Am. Chem. Soc. 104 (1982) 5667;
(c) S.C. Nyburg, A.G. Brook, F. Abdesaken, G. Gutekunst, W. Wong-Ng, Acta Cryst. C 41 (1985) 1632.
[4] (a) A.S. Batsanov, I.M. Clarkson, J.A.K. Howard, P.G. Steel, Tetrahedron Lett. 37 (1996) 2491;
(b) M.B. Berry, R.J. Griffiths, M.J. Sanganee, P.G. Steel, D.K. Whelligan, Tetrahedron Lett. 44 (2003) 9135;
(c) M.B. Berry, R.J. Griffiths, M.J. Sanganee, P.G. Steel, D.K. Whelligan, Org. Biomol. Chem. 2 (2004) 2381;
(d) J.D. Sellars, P.G. Steel, M.J. Turner, Chem. Commun. (2006) 2385;
(e) J.D. Sellars, P.G. Steel, Org. Biomol. Chem. 4 (2006) 3223.
[5] G. Bertrand, J. Dubac, P. Mazerolles, J. Ancelle, J. Chem. Soc. Chem. Commun. (1980) 382.
[6] (a) G.A. Showell, J.S. Mills, Drug Discov. Today 8 (2003) 551;
(b) J.S. Mills, G.A. Showell, Exp. Opin. Invest. Drugs 13 (2004) 1149;
(c) W. Bains, R. Tacke, Curr. Opin. Drug Discov. Dev. (2003) 6526;
(d) P.K. Pooni, G.A. Showell, Mini-Rev. Med. Chem. 6 (2006) 1169.
[7] H. Ottosson, P.G. Steel, Chem. Eur. J. 12 (2006) 1576.
[8] I. El-Sayed, T. Guliashvili, R. Hazell, A. Gogoll, H. Ottosson, Org. Lett. 4 (2002) 1915.
[9] (a) S. Bailleux, M. Bogey, J. Breidung, H. Bürger, R. Fajgar, Y. Liu, J. Pola, M. Senzlober, W. Thiel, Angew. Chem. Int. Ed. Engl. 35 (1996) 2513;
(b) S. Bailleux, M. Bogey, J. Demaison, H. Burger, M. Senzlober, J. Breidung, W. Thiel, R. Fajgar, J. Pola, J. Chem. Phys. 106 (1997) 10016.
[10] C. Liang, L.C. Allen, J. Am. Chem. Soc. 112 (1990) 1039.
[11] M.W. Schmidt, M.S. Gordon, M. Dupuis, J. Am. Chem. Soc. 107 (1985) 2585.
[12] J.M. Galbraith, E. Blank, S. Shaik, P.C. Hiberty, Chem. Eur. J. 6 (2000) 2425.
[13] A. Nicolaides, W.T. Borden, J. Am. Chem. Soc. 113 (1991) 6750.
[14] J. Breidung, W. Thiel, Theor. Chem. Acc. 100 (1998) 183.
[15] N. Auner, J. Grobe, T. Müller, H.W. Rathmann, Organometallics 19 (2000) 3476.
[16] H. Friebolin, Basic One- and Two-Dimensional NMR Spectroscopy, VCH, Weinheim, 1993.
[17] G. Maier, G. Mihm, H.P. Reisenauer, Angew. Chem. Int. Ed. Engl. 20 (1981) 597.
[18] P.A. Snyder, S. Atanasova, J. Phys. Chem. A 108 (2004) 4194.
[19] P. Rosmus, H. Bock, M. Soluki, G. Maier, G. Mihm, Angew. Chem. Int. Ed. Engl. 20 (1981) 598.
[20] The IP of ethene is 10.52 eV, see: S.G. Lias, Ionization Energy Evaluation and S.G. Lias, J.E. Bartmess, J.F. Liebman, J.L. Holmes, R.D. Levin, W.G. Mallard, Ion Energetics Data, in: W.G. Mallard, P.J. Linstrom (Eds.), NIST Chemistry Webbook, NIST Standard Reference Database Number 69, July 2001, National Institute of Standards and Technology, Gaitherburg, MD (http://webbook.nist.gov).
[21] (a) D.E. Goldberg, D.H. Harris, M.F. Lappert, K.M. Thomas, J. Chem. Soc. Chem. Comm. (1976) 261;
(b) P.J. Davidson, D.H. Harris, M.F. Lappert, J. Chem. Soc., Dalton Trans. (1976) 2268.
[22] D.E. Goldberg, P.B. Hitchcock, M.F. Lappert, K.M. Thomas, A.J. Thorne, T. Fjeldberg, A. Haaland, B.E.R. Schilling, J. Chem. Soc., Dalton Trans. (1986) 2387.
[23] L. Pauling, Proc. Natl. Acad. Sci. U.S.A. 80 (1983) 3871.
[24] W.V. Volland, E.R. Davidson, W.T. Borden, J. Am. Chem. Soc. 101 (1979) 533.
[25] R.G. Pearson, Symmetry Rules for Chemical Reactions: Orbital Topology and Elementary Processes, John Wiley and Sons, New York, 1976.
[26] (a) E.A. Carter, W.A. Goddard III, J. Phys. Chem. 90 (1986) 998;
(b) E.A. Carter, W.A. Goddard III, J. Chem. Phys. 88 (1988) 1752.
[27] W.A. Chupka, C. Lifshitz, J. Chem. Phys. 48 (1968) 1109.
[28] K.F. Zmbov, O.M. Uy, J.L. Margrave, J. Am. Chem. Soc. 90 (1968) 5090.
[29] G. Trinquier, J.-P. Malrieu, J. Am. Chem. Soc. 109 (1987) 5303.
[30] For example tetramesityldisilene displays polymorphism where two crystal forms have pyramidal Si atoms and one has planar Si atoms. See: L.A. Leites, S.S. Bukalov, J.E. Mangette, T.A. Schmedake, R. West, Spectrochim. Acta, Part A 59 (2003) 1975.
[31] G. Trinquier, J. Am. Chem. Soc. 112 (1990) 2130.
[32] J.-P. Malrieu, G. Trinquier, J. Am. Chem. Soc. 111 (1989) 5916.
[33] A. Sekiguchi, T. Tanaka, M. Ichinohe, K. Akiyama, S. Tero-Kubota, J. Am. Chem. Soc. 125 (2003) 4962.
[34] P.P. Gaspar, R. West, in: Z. Rappoport, Y. Apeloig (Eds.), The Chemistry of Organic Silicon Compounds II, vol. 2 (Part 3), John Wiley and Sons Ltd., New York, 1998 (Chapter 43).
[35] Y. Apeloig, R. Pauncz, M. Karni, R. West, W. Steiner, D. Chapman, Organometallics 22 (2003) 3250.
[36] H. Jacobsen, T. Ziegler, J. Am. Chem. Soc. 116 (1994) 3667.
[37] H.-J. Himmel, H. Schnöckel, Chem. Eur. J. 9 (2003) 748.
[38] (a) W. Kutzelnigg, Angew. Chem. Int. Ed. Engl. 23 (1984) 272;
(b) G. Raabe, J. Michl, Chem. Rev. 85 (1985) 419.
[39] (a) R. Becerra, R. Walsh, in: Z. Rappoport, Y. Apeloig (Eds.), The Chemistry of Organosilicon Compounds, vol. 2, Wiley, Chichester, 1998, p. 153 (Chapter 4);
(b) R. Walsh, in: S. Patai, Z. Rappoport (Eds.), The Chemistry of Organosilicon Compounds, vol. 1, Wiley, Chichester, 1989, p. 371 (Chapter 5).
[40] R. Grev, Adv. Organomet. Chem. 33 (1991) 125.
[41] J. Grunenberg, Angew. Chem. Int. Ed. 40 (2001) 4027.
[42] (a) R. Stegmann, G. Frenking, J. Comput. Chem. 17 (1996) 781;
(b) Y. Apeloig, M. Karni, Organometallics 16 (1997) 310.
[43] (a) A.D. Becke, K.E. Edgecombe, J. Chem. Phys. 92 (1990) 5397;
(b) A. Savin, R. Nesper, S. Wengert, T.F. Fässler, Angew. Chem. Int. Ed. Engl. 36 (1997) 1809.
[44] H. Grützmacher, T.F. Fässler, Chem. Eur. J. 6 (2000) 2317.
[45] R.F.W. Bader, Chem. Rev. 91 (1991) 893.
[46] N.O.J. Malcolm, R.J. Gillispie, P.L.A. Popelier, J. Chem. Soc., Dalton Trans. (2002) 3333.
[47] D. Bourrisou, O. Guerret, F.P. Gabbai, G. Bertrand, Chem. Rev. 100 (2000) 39.
[48] (a) M.C. Holthausen, W. Koch, Y. Apeloig, J. Am. Chem. Soc. 121 (1999) 2623;
(b) M. Yoshida, N. Tamaoki, Organometallics 21 (2002) 2587.
[49] (a) L.E. Gusel'nikov, V.G. Avakyan, S.L. Gusel'nikov, Russ. J. Gen. Chem. 12 (2001) 2040;
(b) L.E. Gusel'nikov, V.G. Avakyan, S.L. Guselnikov, J. Am. Chem. Soc. 124 (2002) 662;
(c) V.G. Avakyan, S.L. Guselnikov, L.E. Gusel'nikov, J. Organomet. Chem. 686 (2003) 257.
[50] Y. Apeloig, M. Karni, J. Am. Chem. Soc. 106 (1984) 6676.
[51] M.-J. Cheng, S.-Y. Chu, Organometallics 24 (2005) 3746.
[52] J.E. Huhey, Inorganic Chemistry, Principles of Structures and Reactivity, 3rd ed., Harper & Row, New York, 1983, pp. 260–262.
[53] A.P. Scott, I. Agranat, P.U. Biedermann, N.V. Riggs, L. Radom, J. Org. Chem. 62 (1997) 2026, and references cited therein.
[54] H. Möllerstedt, M.C. Piqueras, R. Crespo, H. Ottosson, J. Am. Chem. Soc. 126 (2004) 13938.
[55] (a) G.W. Schriver, M.J. Fink, M.S. Gordon, Organometallics 6 (1987) 1977;
(b) S.M. Bachrach, M. Liu, J. Org. Phys. Chem. 4 (1991) 242;
(c) P. Burk, J.-L. Abboud, I.A. Koppel, J. Phys. Chem. 100 (1996) 6992.
[56] K. Sakamoto, J. Ogasawara, H. Sakurai, M. Kira, J. Am. Chem. Soc. 119 (1997) 3405.
[57] (a) T. Veszprémi, M. Takahashi, J. Ogasawara, K. Sakamoto, M. Kira, J. Am. Chem. Soc. 120 (1998) 2408;
(b) T. Veszprémi, M. Takahashi, B. Hajgató, J. Ogasawara, K. Sakamoto, M. Kira, J. Phys. Chem. A 102 (1998) 10530;
(c) M. Takahashi, K. Sakamoto, M. Kira, Int. J. Quant. Chem. 84 (2001) 198.

[58] K. Sakamoto, J. Ogasawara, Y. Kon, T. Sunagawa, C. Kabuto, M. Kira, Angew. Chem. Int. Ed. 41 (2002) 1402.
[59] H. Ottosson, unpublished results.
[60] For H_3Si^- an E_{inv} of 23.87 kcal/mol has been calculated at the CCSD(T)-R12/[16s11p6d5f/7s5p4d] level with additional corrections for core correlation, special relativity, and diagonal Born–Oppenheimer correction: K. Aarset, A.G. Csaszar, E.L. Sibert III, W.D. Allen, H.F. Schaefer III, W. Klopper, J. Noga, J. Chem. Phys. 112 (2000) 4053.
[61] The $\sum\alpha$(Si) of F_3Si^- is found in the range 289.8–292.5° with a set of different DFT methods. See: J.D. Larkin, C.W. Bock, H.F. Schaefer III, J. Phys. Chem. A 109 (2005) 10100.
[62] (a) S. Saebø, S. Stroble, W. Collier, R. Ethridge, Z. Wilson, M. Tahai, C.U. Pittman Jr, J. Org. Chem. 64 (1999) 1311;
(b) W. Collier, S. Saebø, C.U. Pittman Jr., J. Mol. Struct. (Theochem) 549 (2001) 1.
[63] The nucleus independent chemical shifts at 1.0 Å separation from the ring and calculated at B3LYP/tsV + 2P level reported in reference 57b are −2.1 (**14**), −4.2 (**15**), and −6.8 (**16**) ppm.
[64] H. Ottosson, Chem. Eur. J. 9 (2003) 4144.
[65] (a) R. Walsh, Organometallics 8 (1989) 1973;
(b) R. Walsh, Pure Appl. Chem. 59 (1987) 69.
[66] H.S. Gutowsky, J. Chen, P.J. Hajduk, J.D. Keen, C. Chuang, T. Emilsson, J. Am. Chem. Soc. 113 (1991) 4747.
[67] N. Wiberg, G. Wagner, G. Muller, Angew. Chem. Int. Ed. Engl. 24 (1985) 229.
[68] Y. Apeloig, M. Bendikov, M. Yuzefovich, M. Nakash, D. Bravo-Zhivotovskii, J. Am. Chem. Soc. 118 (1996) 12228.
[69] S. Inoue, M. Ichinohe, A. Sekiguchi, Angew. Chem. Int. Ed. 46 (2007) 3346.
[70] W.M. Boesveld, B. Gehrhus, P.B. Hitchcock, M.F. Lappert, P.v.R. Schleyer, Chem. Commun. (1999) 755.
[71] M. Kaftory, M. Kapon, M. Botoshansky, in: Z. Rappoport, Y. Apeloig (Eds.), The Chemistry of Organic Silicon Compounds, vol. 2, Wiley, Chichester, 1998, p. 181.
[72] J. Ohshita, S. Masaoka, Y. Masaoka, H. Hasebe, M. Ishikawa, Organometallics 15 (1996) 3136.
[73] T. Guliashvili, I. El-Sayed, A. Fischer, H. Ottosson, Angew. Chem. Int. Ed. 42 (2003) 1640.
[74] G. Berthier, J. Serre, in: S. Patai (Ed.), The Chemistry of the Carbonyl Group, vol. 1, Wiley, London, 1966, p. 1.
[75] I. Bejan, D. Güclü, S. Inoue, M. Ichinohe, A. Sekiguchi, D. Scheschkewitz, Angew. Chem. Int. Ed. 46 (2007) 3349.
[76] Y. Liu, P.E. Lindner, D.M. Lemal, J. Am. Chem. Soc. 121 (1999) 10626.
[77] F.E. Hahn, L. Wittenbecher, D. Le Van, R. Fröhlich, Angew. Chem. Int. Ed. 112 (2000) 541.
[78] C.E. Allison, T.B. McMahon, J. Am. Chem. Soc. 112 (1990) 1672.
[79] (a) R. Benassi, C. Bertini, E. Kleinpeter, F. Taddei, J. Mol. Struct. (Theochem) 498 (2000) 217;
(b) R. Benassi, C. Bertarini, F. Taddei, E. Kleinpeter, J. Mol. Struct. (Theochem) 541 (2001) 101;
(c) R. Benassi, F. Taddei, J. Mol. Struct. (Theochem) 572 (2001) 169.
[80] (a) S.Y. Wang, W.T. Borden, J. Am. Chem. Soc. 111 (1989) 7282;
(b) E.C. Wu, A.S. Rodgers, J. Am. Chem. Soc. 98 (1976) 6112.
[81] W.-C. Chen, M.-D. Su, S.-Y. Chu, Organometallics 20 (2001) 564.
[82] (a) The rotational barrier of $H_3Si–CH_3$ at MP2/6-31G(d) level is 1.88 kcal/mol and the experimental value is 1.7 kcal/mol: P.v.R. Schleyer, M. Kaupp, F. Hampel, M. Bremer, K. Mislow, J. Am. Chem. Soc. 114 (1992) 6791;
(b) C. Pouchan, G. Lespes, A. Darbelos, J. Phys. Chem. 92 (1988) 28.
[83] A.G. Brook, F. Abdesaken, G. Gutekunst, N. Plavac, Organometallics 1 (1982) 994.
[84] K.M. Baines, A.G. Brook, R.R. Ford, P.D. Lickiss, A.K. Saxena, W.J. Chatterton, J.F. Sawyer, B.A. Behnam, Organometallics 8 (1989) 693.
[85] N. Wiberg, G. Wagner, G. Mueller, Angew. Chem. Int. Ed. Engl. 24 (1985) 229.
[86] A.G. Brook, A. Baumegger, A.J. Lough, Organometallics 11 (1992) 3088.
[87] I.S. Toulokhonova, I.A. Guzei, R. West, J. Am. Chem. Soc. 126 (2004) 5336.
[88] (a) G. Delpon-Lacaze, C. Couret, J. Organomet. Chem. 480 (1994) C14;
(b) G. Delpon-Lacaze, C. de Battisti, C. Couret, J. Organomet. Chem. 514 (1996) 59.
[89] A. Sekiguchi, M. Nanjo, C. Kabuto, H. Sakurai, Organometallics 14 (1995) 2630.
[90] C. Kayser, R. Fischer, J. Baumgartner, C. Marschner, Organometallics 21 (2002) 1023.
[91] B. Gehrhus, P.B. Hitchkock, M.F. Lappert, J. Heinicke, R. Boese, D. Bläser, J. Organomet. Chem. 521 (1996) 211.
[92] J.J. Buffy, R. West, M. Bendikov, Y. Apeloig, J. Am. Chem. Soc. 123 (2001) 978.
[93] The chemical shift anisotropy (CSA) is defined as $\delta_{11} - [(\delta_{22} + \delta_{33})/2]$ with δ_{11}, δ_{22}, and δ_{33} being the chemical shielding tensor components.
[94] H.-P. Reisenauer, G. Mihm, G. Maier, Angew. Chem. Int. Ed. Engl. 21 (1982) 854.
[95] W.J. Leigh, R. Boukherroub, C. Kerst, J. Am. Chem. Soc. 120 (1998) 9504.
[96] G. Mihm, H.P. Reisenauer, D. Littman, G. Maier, Chem. Ber. 117 (1984) 2369.
[97] A. Sekiguchi, W. Ando, Organometallics 6 (1987) 1857.
[98] G. Maier, H. Mihm, H.P. Reisenauer, Chem. Ber. 117 (1984) 2351.
[99] V.N. Khabashesku, V. Balaji, S.E. Bogonov, O.M. Nefedov, J. Michl, J. Am. Chem. Soc. 116 (1994) 320.
[100] M. Trommer, Ph.D. Dissertation, Ruhr-Universität zu Bochum, Bochum, Germany, 1995.
[101] W.J. Leigh, C.J. Bradaric, C. Kerst, J.H. Banisch, Organometallics 15 (1996) 2246.
[102] T.R. Owens, C.R. Harrington, T.C.S. Pace, W.J. Leigh, Organometallics 22 (2003) 5518.
[103] R.T. Conlin, P.F. Mcgarry, J.C. Scaiano, S. Zhang, Organometallics 11 (1992) 2317.
[104] (a) C.J. Braderic, W.J. Leigh, Organometallics 17 (1998) 645;
(b) W.J. Leigh, R. Boukherroub, C.J. Braderic, C.C. Cserti, J.M. Schmiesser, Can. J. Chem. 77 (1999) 1136.
[105] G. Raabe, H. Vancik, R. West, J. Michl, J. Am. Chem. Soc. 108 (1986) 671.
[106] (a) V.V. Volkova, V.G. Avakyan, N.S. Nametkin, L.E. Guselnikov, J. Organomet. Chem. 201 (1980) 137;
(b) O.M. Nefedov, A.K. Maltsev, V.N. Khabashesku, V.A. Korolev, J. Organomet. Chem. 201 (1980) 123.
[107] R. Withnall, L. Andrews, J. Phys. Chem. 92 (1988) 594.
[108] (a) C.-C. Chang, J. Kolc, M.E. Jung, J.A. Lowe, O.L. Chapman, J. Am. Chem. Soc. 98 (1976) 7846;
(b) M.R. Chedekel, M. Skoglund, R.L. Kreeger, H. Shechter, J. Am. Chem. Soc. 98 (1976) 7846.
[109] (a) L.E. Gusel'nikov, N.S. Nametkin, J. Organomet. Chem. 169 (1979) 155;
(b) T. Koenig, W. Mckenna, J. Am. Chem. Soc. 103 (1981) 1212;
(c) J.M. Dyke, G.D. Josland, R.A. Lewis, A. Morris, J. Phys. Chem. 86 (1982) 2913;
(d) H. Bock, R.H. Bowling, B. Solouki, T.J. Barton, G.T. Burns, J. Am. Chem. Soc. 102 (1980) 429;
(e) H. Bock, P. Rosmus, B. Solouki, G. Maier, J. Organomet. Chem. 271 (1984) 145.
[110] M. Bendikov, B. Solouki, N. Auner, Y. Apeloig, Organometallics 21 (2002) 1349.
[111] S.G. Lias, in: W.G. Mallard, P.J. Linstrom (Eds.), Ionization Energy Evaluation, NIST Chemistry WebBook, NIST Standard Reference Database Number 69, July 2001, National Institute of Standards and Technology, Gaitersburg, MD (http://webbook.nist.gov).
[112] M. Bendikov, V. Kravchenko, Y. Apeloig, J.Y. Becker, Organometallics 23 (2004) 921.
[113] B. Cetinkaya, G.H. King, S.S. Krishnamurthy, M.F. Lappert, J.B. Pedley, Chem. Commun. (1971) 1370.
[114] A. Venturini, F. Bernardi, M. Olivucci, M.A. Robb, I. Rossi, J. Am. Chem. Soc. 120 (1998) 1912.
[115] E.T. Seidl, R.S. Grev, H.F. Schaefer III, J. Am. Chem. Soc. 114 (1992) 3643.

[116] Y. Apeloig, D. Bravo-Zhivotovskii, I. Zharov, V. Panov, W.J. Leigh, G.W. Sluggett, J. Am. Chem. Soc. 120 (1998) 1398.
[117] D. Bravo-Zhivotovskii, V. Braude, A. Stanger, M. Kapon, Y. Apeloig, Organometallics 11 (1992) 2326.
[118] (a) C. Krempner, H. Reinke, H. Oehme, Chem. Ber. 128 (1995) 143;
(b) C. Krempner, H. Reinke, H. Oehme, Chem. Ber. 128 (1995) 1083;
(c) F. Luderer, H. Reinke, H. Oehme, Chem. Ber. 129 (1996) 15;
(d) C. Krempner, H. Reinke, H. Oehme, Angew. Chem. Int. Ed. Engl. 33 (1994) 1615;
(e) D. Hoffmann, H. Reinke, H. Oehme, Z. Naturforsch. 51b (1996) 371.
[119] A.G. Brook, J.W. Harris, J. Lennon, M. El- Sheikh, J. Am. Chem. Soc. 101 (1979) 83.
[120] A.G. Brook, R.M.R. Kallury, Y.C. Poon, Organometallics 1 (1982) 987.
[121] D. Bravo-Zhivotovskii, Y. Apeloig, Y. Ovchinnikov, V. Igonin, Y.T. Struchkov, J. Organomet. Chem. 446 (1993) 123.
[122] N. Wiberg, G. Wagner, G. Müller, J. Reine, J. Organomet. Chem. 271 (1984) 381.
[123] N. Wiberg, J. Organomet. Chem. 315 (1984) 9.
[124] H. Sakurai, in: Z. Rappoport, Y. Apeloig (Eds.), The Chemistry of Organic Silicon Compounds, vol. 2, Wiley and Sons, Ltd., New York, 1998, pp. 827–855.
[125] M. Kira, T. Maruyama, H. Sakurai, J. Am. Chem. Soc. 113 (1991) 3986.
[126] W.J. Leigh, T.R. Owens, M. Bendikov, S.S. Zade, Y. Apeloig, J. Am. Chem. Soc. 128 (2006) 10772.
[127] M. Ichinoe, T. Tanaka, A. Sekiguchi, Chem. Lett. (2001) 1074.
[128] T.L. Morkin, W.J. Leigh, Acc. Chem. Res. 34 (2001) 129.
[129] C. Kerst, R. Boukherroub, W.J. Leigh, J. Photochem. Photobiol. A 110 (1997) 243.
[130] W.J. Leigh, C. Kerst, R. Boukherroub, T.L. Morkin, S.I. Jenkins, K. Sung, T.T. Tidwell, J. Am. Chem. Soc. 121 (1999) 4744.
[131] T.L. Morkin, W.J. Leigh, T.T. Tidwell, A.D. Allen, Organometallics 20 (2001) 5707.
[132] M. Bendikov, S.R. Quadt, O. Rabin, Y. Apeloig, Organometallics 21 (2002) 3930.
[133] N. Sewald, W. Ziche, A. Wolff, N. Auner, Organometallics 12 (1993) 4123.
[134] N. Auner, C.-R. Heikenwälder, W. Ziche, Chem. Ber. 126 (1993) 2177.
[135] (a) W. Ziche, N. Auner, J. Behm, Organometallics 11 (1992) 2494;
(b) N. Auner, C. Wagner, W. Ziche, Z. Naturforsch. 49b (1994) 831.
[136] (a) P.R. Jones, T.F.O. Lim, R.A. Pierce, J. Am. Chem. Soc. 102 (1980) 4970;
(b) N. Auner, Z. Anorg. Allg. Chem. 55 (1988) 558.
[137] N. Wiberg, G. Preiner, G. Wagner, H. Köpf, Z. Naturforsch. 42b (1987) 1062.
[138] A.G. Brook, K. Vorspohl, R.R. Ford, M. Hesse, W.J. Chatterton, Organometallics 6 (1987) 2128.
[139] S.S. Al-Juaid, Y. Derouiche, P.B. Hitchcock, P.D. Lickiss, A.G. Brook, J. Organomet. Chem. 403 (1991) 293.
[140] J. Ohshita, S. Masaoka, Y. Morimoto, M. Sano, Organometallics 16 (1997) 1123.
[141] N. Wiberg, K. Schurz, G. Fischer, Chem. Ber. 119 (1986) 3498.
[142] G.E. Miracle, J.L. Ball, D.R. Powell, R. West, J. Am. Chem. Soc. 115 (1993) 11598.
[143] K. Krogh-Jespersen, J. Comput. Chem. 3 (1982) 571.
[144] M. Trommer, G.E. Miracle, B.E. Eichler, D.R. Powell, R. West, Organometallics 16 (1997) 5737.
[145] N. Sigal, Y. Apeloig, Organometallics 21 (2002) 5486.
[146] (a) N. Takeda, H. Suzuki, N. Tokitoh, R. Okazaki, S. Nagase, J. Am. Chem. Soc. 119 (1997) 1456;
(b) N. Takeda, T. Kajiwara, H. Suzuki, R. Okazaki, N. Tokitoh, Chem. Eur. J. 9 (2003) 3530.
[147] T. Abe, T. Iwamoto, C. Kabuto, M. Kira, J. Am. Chem. Soc. 128 (2006) 4228.
[148] (a) M.A. Fernandes, M. Layh, B. Omondi, Acta Crystallogr. C 58 (2002) 384;
(b) T. Mathieson, A. Schier, H. Schmidbaur, J. Chem. Soc., Dalton, Trans. (2001) 1196.
[149] G. Maier, H.P. Reisenauer, H. Egenolf, Organometallics 18 (1999) 2155.
[150] C.A. Arrington, J.T. Petty, S.E. Payne, W.C.K. Haskins, J. Am. Chem. Soc. 110 (1988) 6240.
[151] H. Bornemann, W. Sander, J. Organomet. Chem. 641 (2002) 156.
[152] G. Maier, G. Mihm, H.P. Reisenauer, D. Littman, Chem. Ber. 117 (1984) 2369.